Cell

Manipulating the Selection Forces during Affinity Maturation to Generate Cross-Reactive HIV Antibodies

Graphical Abstract

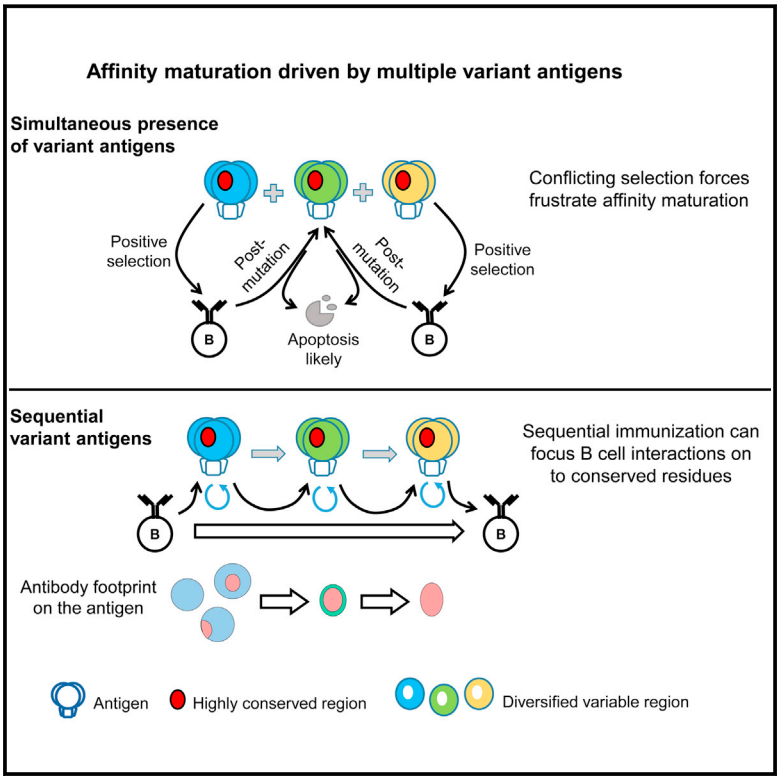

Highlights

- In silico model of affinity maturation driven by variant antigens
- Conflicting selection forces due to antigen variants can frustrate maturation
- Key variables that control evolution of cross-reactive antibodies identified
- Sequential immunization favored for inducing cross-reactive antibodies

Authors

Shenshen Wang, Jordi Mata-Fink, ..., Mehran Kardar, Arup K. Chakraborty

Correspondence

arupc@mit.edu

In Brief

In silico model of antibody affinity maturation explains why antibodies capable of cross-reacting with different variants of viral antigens are uncommon and shows that sequential immunization is effective at inducing cross-reactive HIV antibodies focused on the shared CD4 binding site.

Wang et al., 2015, Cell *160*, 785–797
February 12, 2015
http://dx.doi.org/10.1016/j.cell.2015.01.027

CellPress

Cell

Manipulating the Selection Forces during Affinity Maturation to Generate Cross-Reactive HIV Antibodies

Shenshen Wang,[1,2,3] Jordi Mata-Fink,[1,2] Barry Kriegsman,[2] Melissa Hanson,[5] Darrell J. Irvine,[1,5,8] Herman N. Eisen,[8,9] Dennis R. Burton,[1,4,10] K. Dane Wittrup,[2,5,10] Mehran Kardar,[3,10] and Arup K. Chakraborty[1,2,3,5,6,7,10,*]
[1]Ragon Institute of MGH, MIT, and Harvard, Cambridge, MA 02139
[2]Department of Chemical Engineering, Massachusetts Institute of Technology, Cambridge, MA 02139
[3]Department of Physics, Massachusetts Institute of Technology, Cambridge, MA 02139
[4]Department of Immunology and Microbial Science, The Scripps Research Institute, La Jolla, CA 92037
[5]Department of Biological Engineering, Massachusetts Institute of Technology, Cambridge, MA 02139
[6]Department of Chemistry, Massachusetts Institute of Technology, Cambridge, MA 02139
[7]Institute for Medical Engineering and Science, Massachusetts Institute of Technology, Cambridge, MA 02139
[8]Koch Institute for Integrative Cancer Research, Massachusetts Institute of Technology, Cambridge, MA 02139
[9]Department of Biology, Massachusetts Institute of Technology, Cambridge, MA 02139
[10]Co-senior author
*Correspondence: arupc@mit.edu
http://dx.doi.org/10.1016/j.cell.2015.01.027

SUMMARY

Generation of potent antibodies by a mutation-selection process called affinity maturation is a key component of effective immune responses. Antibodies that protect against highly mutable pathogens must neutralize diverse strains. Developing effective immunization strategies to drive their evolution requires understanding how affinity maturation happens in an environment where variants of the same antigen are present. We present an in silico model of affinity maturation driven by antigen variants which reveals that induction of cross-reactive antibodies often occurs with low probability because conflicting selection forces, imposed by different antigen variants, can frustrate affinity maturation. We describe how variables such as temporal pattern of antigen administration influence the outcome of this frustrated evolutionary process. Our calculations predict, and experiments in mice with variant gp120 constructs of the HIV envelope protein confirm, that sequential immunization with antigen variants is preferred over a cocktail for induction of cross-reactive antibodies focused on the shared CD4 binding site epitope.

INTRODUCTION

Antibodies (Abs) with high affinity for antigen are produced by the process of affinity maturation (AM), which takes place in germinal centers (GCs). GCs are dynamic structures within secondary lymphoid tissues that arise in response to antigen stimulation (Shlomchik and Weisel, 2012; Victora and Nussenzweig, 2012). GCs house B cells, antigen-specific T helper cells that develop in concert with GC B cells (Baumjohann et al., 2013; Kelsoe, 1996) and antigens presented on follicular dendritic cells (FDCs) (Figure 1A). GC B cells enhance the antigen affinity of their receptors by 10- to 1,000-fold through cycles of mutation and selection against antigens presented on FDCs, a Darwinian evolutionary process that occurs on a very short timescale. Soluble forms of the high-affinity receptors are potent Abs. AM has been studied extensively using diverse experimental methods (Batista and Neuberger, 1998; Berek and Milstein, 1987; Berek et al., 1991; Eisen and Siskind, 1964; Jacob et al., 1991; Kocks and Rajewsky, 1988), mathematical models (Deem and Lee, 2003; Kepler and Perelson, 1993; Meyer-Hermann, 2002, Meyer-Hermann et al., 2006; Oprea and Perelson, 1997; Zhang and Shakhnovich, 2010), and computer simulations (Keşmir and De Boer, 2003; Shlomchik et al., 1998; Swerdlin et al., 2008). Recent experiments have uncovered new aspects of GC dynamics (Allen et al., 2007; Shulman et al., 2013; Victora et al., 2010).

Effective Ab responses are likely to be required for a protective prophylactic vaccine against highly mutable pathogens. For HIV, a quintessential example of such a pathogen, there has been no definitive success in designing such a vaccine, despite extensive efforts (Burton et al., 2012; Klein et al., 2013; Kwong et al., 2013; Mascola and Haynes, 2013). This is in large part due to the variability of HIV (Burton et al., 2012; Mascola and Haynes, 2013).

The protective effects of an Ab are predicated on its ability to bind to a set of residues (the epitope) on the surface of virions. For example, the HIV-1 envelope glycoprotein trimer (Env) is the sole target of known HIV-1 neutralizing Abs (Burton et al., 2012; Kwong et al., 2013; Mascola and Haynes, 2013; West et al., 2014). During the first few months of infection, the induced neutralizing Abs are primarily strain-specific and target variable regions of Env. As the concentrations of such strain specific Abs increase, neutralization escape variants with mutations in the variable epitopes are selected. A pathogen's molecular

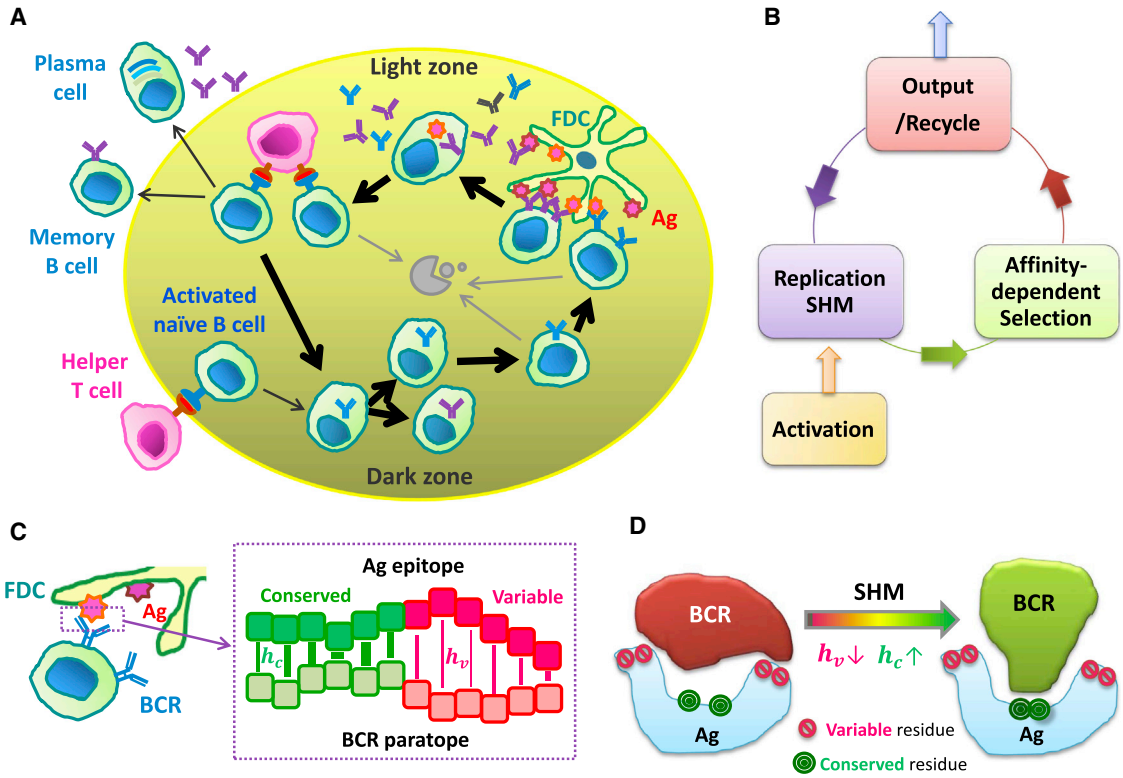

Figure 1. Schematic Depiction of In Silico Model

(A) Players and processes in the GCR.

(B) Major steps in our in silico model of the GCR.

(C) Model for BCR-Ag interactions. Left: A BCR interacting with an FDC-held Ag. Right: A zoom-in view of interactions (bars) between the residues on the BCR paratope and those on the Ag epitope. An affinity-affecting mutation on a paratope residue will change its interaction strength h with the corresponding epitope residue, denoted by h_c (h_v) if the latter is conserved (variable).

(D) Conformational coupling between residues on the BCR is incorporated via correlated changes in h_c and h_v; weakening interaction with the variable residues and the residues that shield the conserved residues of the epitope (red symbols), i.e., $h_v\downarrow$, would facilitate access to the conserved residues (green symbols), i.e., $h_c\uparrow$.

See also Figure S1.

surfaces that interact with host receptors (e.g., the CD4 binding site) provide epitopes that contain a relatively conserved set of residues. They can serve as targets for Abs that are able to neutralize a greater diversity of HIV strains. A shield of glycans and immunodominant variable loops can restrict antibody access to these relatively conserved epitopes (Julien et al., 2013; Kwong et al., 2002; Lyumkis et al., 2013; Pancera et al., 2014; Wei et al., 2003; Wyatt et al., 1998). Yet, some HIV-1 infected individuals do develop Abs that focus on such epitopes and neutralize a broad cross section of HIV strains in vitro (Kwong et al., 2013). However, these broadly neutralizing antibodies (bnAbs) are produced only beginning around 2 years after infection and in only a limited fraction of chronically infected patients. Nonetheless, the emergence of bnAbs in some patients is proof that AM can result in bnAbs. This suggests the tantalizing possibility that appropriately designed immunogens and immunization protocols may be able to elicit bnAbs rapidly in a large fraction of individuals, thus resulting in an effective vaccine.

Recent longitudinal tracking of a developing HIV-1 bnAb lineage and the co-evolving virus in a patient showed that extensive, and even specifically directed, viral diversification occurred prior to the development of breadth (cross-reactive Abs) (Gao et al., 2014; Liao et al., 2013), supporting the idea that escape mutants of the virus drive bnAb evolution. More importantly, this observation highlights that induction of bnAbs will likely require immunization with multiple variants of the antigen.

When multiple complex antigen variants are used as immunogens, several new questions become important, for example: (1) which antigen variants should be used as immunogens; (2) what should be the concentrations and temporal order in which they are administered (e.g., cocktails versus sequential)? The answers to these questions are drawn from a huge number of possibilities, and random selection from a large number of combinations of options may not allow sufficient sampling to find efficacious strategies. Intuition is unlikely to guide choices correctly because a mechanistic understanding of how AM occurs in the face of variant or mutating antigens is not available, as past studies have focused on AM in response to single model antigens. This gap in basic immunobiology needs to be addressed. A fundamental understanding of AM induced by several antigen

variants that mimic the complexity of how conserved epitopes are shielded on the intact viral spike could be harnessed to design optimal immunogens and immunization protocols for the development of universal vaccines against highly mutable pathogens (e.g., HIV-1, influenza).

To take steps toward these goals, we developed an in silico model of AM induced by variant antigens. This stochastic dynamic model enables examination of the key mechanisms and factors that influence AM in the face of variant antigens and the development of bnAbs. Our calculations predict markedly distinct outcomes if designed antigen (Ag) variants are presented in different concentrations and temporal patterns during immunization. Experiments in mice using model HIV antigens are consistent with these predictions. Thus, our complementary computational and experimental results provide broadly applicable fundamental insights, and a guide for further studies aimed at overcoming roadblocks to the induction of bnAbs against HIV-1 by vaccination.

RESULTS

In Silico Model

The purpose of our in silico modeling is not quantitative recapitulation of existing experiments but to provide fundamental mechanistic insights into AM induced by multiple Ag variants and to compare the predicted relative efficacy of different immunization schemes in inducing cross-reactive broadly neutralizing Abs (bnAbs). Two key features not considered before must be incorporated explicitly in such studies; viz., the presence of multiple Ag variants during GC reactions and the molecular complexity of the Ags. To mimic interactions of B cell receptors with complex immunogens such as the HIV-1 trimeric spike, we account for the fact that the conserved protein epitope of desired Abs are partially shielded, and that insertions and deletions in the variable loops can hinder the formation of strong interactions with the conserved residues of the epitopes (e.g., those in the CD4bs).

We computationally simulate the dynamics of a typical GC (Figure 1A). The GC reaction (GCR) starts on day 3 (Nieuwenhuis and Opstelten, 1984) after Ag injection, with three B cell blasts (Jacob et al., 1991; Kroese et al., 1987) that barely meet a relatively low-affinity threshold, E_a. The qualitative results we report do not depend on the particular value of E_a since all other affinities are scaled relative to it. The B cells expand without mutation, reaching a population size of about 1,500 cells around day 7 (Jacob et al., 1991).

Hypermutation in the Dark Zone of the GC

At day 7, AID-mediated somatic hypermutation (SHM) in the immunoglobin (Ig) genes turns on (Källberg et al., 1996) with a rate of 10^{-3} per base pair per division (Berek and Milstein, 1987). Variations in the time at which SHM begins do not affect our results as we start timing AM processes after this point. Each B cell in the dark zone of the GC (the region where this replication/mutation occurs) replicates twice, and we assume that mutation occurs uniformly, neglecting preferential replacements or hypermutation hotspots (Wagner et al., 1995). We assume that the activated B cells are from an appropriate germline (Kepler et al., 2014). The probability of a functionally silent mutation (no change in affinity) is $p_S = 0.5$, the probability that a mutation is lethal (e.g., non-folding) is $p_L = 0.3$, and the rest are affinity-affecting mutations (probability $p_A = 0.2$) (Shlomchik et al., 1998). For affinity-affecting mutations, the affinity of a BCR (i) with a particular type of antigen (j), E_{ij}, is changed. The extent of the change is chosen from a probability distribution characterized by a long tail of deleterious mutations that reduce affinity, as experimental data suggest that favorable mutations are less likely than deleterious ones (Figure S1A). Our BCR-Ag affinity model is defined in a later sub-section.

Selection in the Light Zone of the GC

B cells whose re-expressed surface Ig genes do not carry lethal mutations then go through affinity-dependent selection. Two survival signals are required for a B cell to be positively selected. First, the BCR on a B cell must bind to the Ag (immunogen) displayed on the FDC sufficiently strongly to enable internalization. Since processes occur stochastically, in our simulations, B cells internalize Ag with a probability related to the binding affinity of its BCR for the Ag. The greater the difference between the affinity (E_{ij}) of a B cell (i) for its epitope on Ag j and a threshold (E_a) required for Ag internalization, the greater the probability of Ag internalization. This probability is described mathematically in analogy with a Langmuir isotherm (Equation 1 in Experimental Procedures).

B cells that internalize Ag display antigenic peptides (p) bound to major histocompatibility complex (MHC) molecules on their surface. T cell receptors expressed on T helper cells can bind to these pMHCs to deliver a key survival signal. B cells compete with each other for the limited availability of T cell help (Victora et al., 2010). T helper cells are specific for peptides derived from the Ag, but they are responsive to diverse pMHCs, not just those derived from the epitope targeted by the BCR. Thus, we assume that the probability of a B cell receiving T cell help is dictated by the amount of internalized Ag, regardless of the identity of its targeted epitope. A B cell that successfully internalizes Ag receives T cell help with a probability that depends upon its probability of internalizing Ag relative to the average probability of internalizing Ag of all the other B cells present in the GC (Equation 2 in Experimental Procedures). A B cell with a high affinity for its target epitope competes better for T cell help.

To study AM against Ag variants that may be present simultaneously, we have to confront an issue for which no experimental information exists: when a GC B cell encounters a FDC, with how many types of Ag variants can it simultaneously interact? We consider two scenarios: (1) each GC B cell interacts with one type of Ag variant during an encounter, or (2) each GC B cell interacts simultaneously with all Ag variants held on the FDCs. We find that which of these scenarios describes the heterogeneity of Ag display on FDCs strongly influences the outcome of AM, indicating the importance of experimental interrogation of this issue.

We study two extreme cases of competition for T cell help: (1) GC B cells compete only with contemporary GC B cells (“peers only”) and (2) in addition to current GC B cells, all antibodies generated in previous rounds of mutation/selection also participate in the competition (“Ab feedback”). Reality should be bounded by these scenarios.

Recycling, Differentiation, and Termination of the GCR

From seminal studies (Oprea and Perelson, 1997), 90% of the selected cells are recirculated to the dark zone. The rest

differentiate into equal numbers of Ab-secreting plasma cells and memory cells that can re-expand upon future activation. Ab feedback is provided by objects in our agent-based model with affinities representing these past GC emigrants. As AM proceeds, at first, the number of B cells in the GC decreases. In some cases, all B cells apoptose and the GC extinguishes. In others, upon reaching a population bottleneck, favorable clones emerge, and the number of B cells rises (Zhang and Shakhnovich, 2010). We terminate the GCR once the GC population recovers to the initial size (i.e., ~1,500 cells), or when an assumed maximum duration of 120 days (or 240 GCR cycles) is reached, whichever comes first. The first condition reflects the fact that an abundance of GC B cells will internalize all the Ag on FDCs. The second condition may reflect antigen decay over time which we do not model explicitly.

Model for BCR-Ag Affinity

In classic computational studies focused on GCR stimulated by a single model Ag, B cells were binned into different affinity classes for the Ag (e.g., Kepler and Perelson, 1993). The correlated affinities for different Ag variants require a more detailed description. Other studies have considered mathematical models (such as NK-models) for BCR properties and their Ag affinity that present rugged landscapes for affinity evolution (Deem and Lee, 2003). To unambiguously define affinity to different Ag variants and to consider complex immunogens that reflect features on viral spikes, we developed a coarse-grained model with "residue-level" resolution for key BCR-Ag interactions (Figure 1C). Our model was inspired by the CD4bs on the trimeric HIV-1 viral spike, which is targeted by many monoclonal bnAbs for HIV-1 (Burton et al., 2012). But, it applies to other epitopes that contain highly conserved residues and can easily be modified to consider other pathogens. We ignore distracting epitopes that do not contain conserved residues because they are less likely to elicit bnAbs.

BCRs can potentially make contacts with three types of residues on the viral spike: (1) highly conserved residues of the epitope (18 such residues in model); (2) residues representing motifs, such as glycan attachment sites, which, when occupied, can be associated with sterically blocking access to the conserved residues (6 such residues in model); and (3) variable residues, which upon mutation (includes insertions/deletions), can further mask the conserved residues of the epitope. We include 22 such residues from the variable loops of Env that mimic the most mutable sites in the Seaman neutralization test panel (Seaman et al., 2010; Walker et al., 2011) sequences and publicly available Env sequences.

Each epitope residue is described in a coarse grained manner, such that it is either the wild-type (WT) amino acid or a mutant. The strength of interaction of a residue (k) on BCR (i) with a residue on the epitope is denoted by h^i_k. The binding affinity, E_{ij}, between a B cell clone $\vec{h}^i$ and a viral strain $\vec{s}^j$ is modeled as

$$E_{ij}\left(\vec{h}^i, \vec{s}^j\right) = \sum_{k=1}^{M} h^i_k s^j_k + \sum_{k=M+1}^{N} h^i_k. \quad (1)$$

The first M interactions (i.e., $k \leq M$) are with variable contact residues on the viral spike, where s_k can be either 1 (WT) or −1 (mutated). The other ($N-M$) sites (i.e., $k>M$) are conserved residues on the epitope with $s_k = 1$. The interaction strength h_k is drawn from a continuous and uniform distribution within a bounded range (details in "Simulation Methods" in Extended Experimental Procedures).

Equation 1 is, however, just a starting point for the affinity between a particular BCR and Ag, as BCRs do not interact with peptide chains in a linear fashion, and interactions between residues are not independent, as Equation 1 may imply. Epitope-paratope interactions are distinctly 3-dimensional, and structural aspects of CD4bs bnAbs also point to the importance of how interactions with some residues on the viral spike might influence interactions with other epitope residues (Zhou et al., 2010). For instance, most CD4bs bnAbs avoid contact with almost the entire V1/V2 loop except for a few conserved residues near the stem, and the very potent VRC01 Ab avoids the V5 loop. This suggests that avoiding interactions with some residues can allow better access and stronger interactions with the conserved residues of the epitope. Furthermore, affinity enhancement of bnAbs (such as VRC01) is influenced by alteration of non-contact residues (Klein et al., 2013). We account for these effects as described below (mathematical details in "Simulation Methods" in Extended Experimental Procedures).

BCR mutations that strengthen (weaken) interactions with the residues that shield the conserved residues could result in a decreased (increased) binding strength (value of h in Equation 1) for a randomly chosen paratope residue that can potentially interact with a conserved residue on the epitope. This feature reflects the fact that BCRs that decrease contacts with shielding residues are more likely to be able to access and make contacts with the protected conserved residues.

Current knowledge on Env structures (Julien et al., 2013; Lyumkis et al., 2013; Pancera et al., 2014) indicates that V1 is likely to be a dynamic, unfolded, and disordered flexible loop, and mutations in V2, especially insertions/deletions, can hide the conserved residues of a neutralizing epitope. So, paratope alterations that weaken interaction with a mutated variable loop residue result in an increased binding strength (value of h in Equation 1) for a randomly chosen paratope residue that can potentially interact with a conserved residue on the epitope (Figure 1D), and vice versa.

Choice of Immunogens and Immunization Schemes

In silico, we study three Ag variants, the WT Ag (only unmutated residues) and two mutants. Of the 22 most mutable residues in the variable loops, 20 residues are mutated in the majority of the 141 Seaman test panel sequences (Figure S1B). As these highly mutated strains are viable, to maximize the number of non-overlapping mutated residues on the Ag variants, we studied two mutant strains with 11 non-overlapping mutations in the variable sites. We also studied variants with 4 and 8 such mutations. We assume that these Ag variants are not so distal in sequence space that they stimulate completely different B cell lineages.

We investigate three immunization schemes in silico: (1) scheme I (WT+v1+v2): WT Ag and two variants administered as a cocktail. (2) scheme II (WT|v1+v2): Immunization with WT Ag first, followed by administration of the two variants simultaneously. (3) scheme III (WT|v1|v2): Immunization with WT Ag first, followed by sequential administration of the two variants. In our murine experiments we studied schemes I and III.

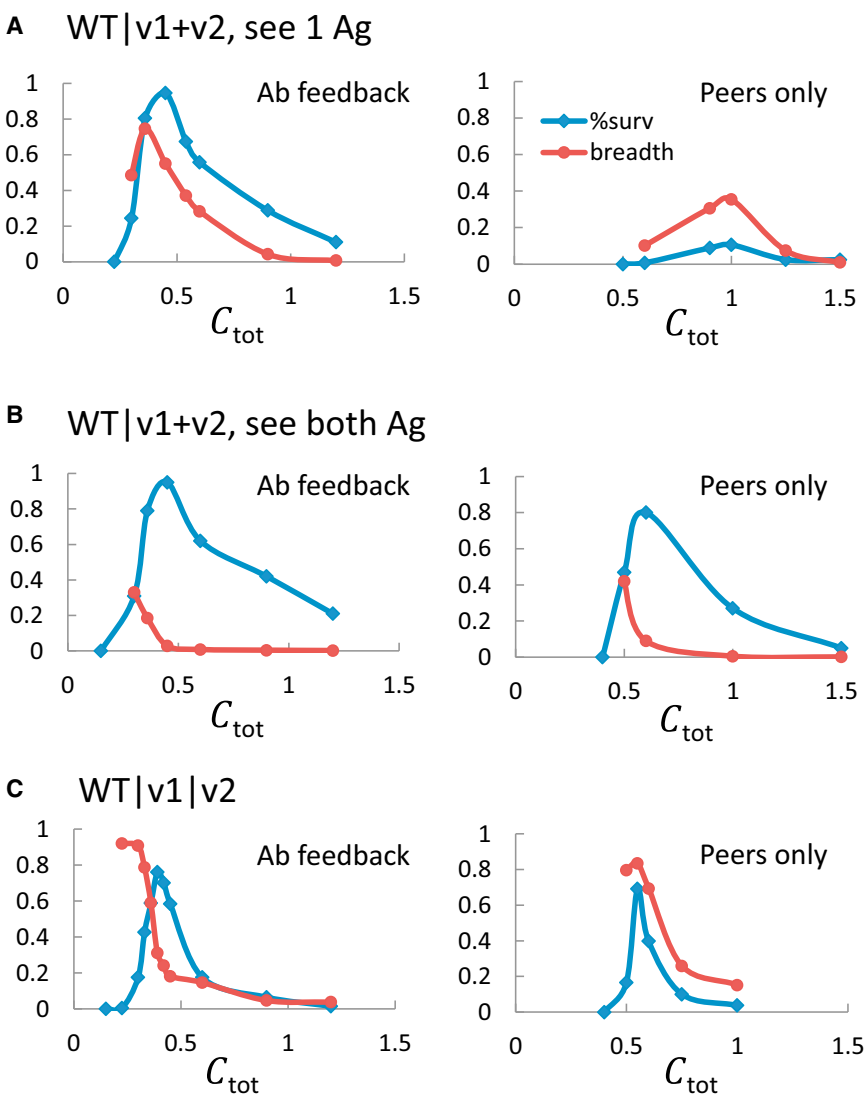

Figure 2. Concentration Dependence of GC Survival and Antibody Breadth in "WT First" Schemes

(A–C) For a relevant range of Ag concentrations (C_{tot}), the fraction of surviving GCs (%surv, blue) and their Ab breadth (red) are shown for (A) scheme II (see 1 Ag), (B) scheme II (see both Ag) and (C) scheme III, with full (left column) or none (right column) Ab feedback. See also Figures S2 and S3.

For each immunization protocol, we simulate many GC reactions. When all steps of immunization and AM are completed, we check whether the affinity of each Ab produced by a GC exceeds a threshold value against each strain in the Seaman panel. Thus, we assess the breadth of cross-reactivity. The breadth of coverage is defined as the fraction of test panel sequences to which an Ab binds with an above-threshold affinity. We collect statistics from many Abs and simulations, and report results as histograms or probabilities of obtaining Abs with a certain breadth. As many GCs are induced in each vaccinated person, these results reflect the probability of obtaining Abs that exhibit particular breadths of coverage in a typical individual.

Model Reproduces Known Features of Affinity Maturation with a Single Antigen

Immunization with only the WT Ag leads to affinity enhancement on conserved and variable residues alike (Figure S1E). The number of accumulated mutations (seven affinity-affecting mutations in 2 weeks, Figure S1D) and the incremental changes in interaction strength (Figure S1E) are consistent with experiment (Berek et al., 1991; Kocks and Rajewsky, 1988; Wedemayer et al., 1997). Higher affinity clones continuously emerge, producing potent Abs (Figure S2 C and F).

The Effect of Antigen Concentration

For a single Ag, if Ag dose is too low (Figures S2A–S2B and S2D–S2E, lowest C_{wt}), B cells are unlikely to be selected during GC reactions, the GC collapses, and there is no Ab production. If Ag dose is too high (Figures S2A–S2B and S2D–S2E, highest C_{wt}), selection is easy, there is little competition between B cells, and GCs are rapidly filled with low-affinity clones (Eisen and Siskind, 1964; Goidl et al., 1968). Our agent-based stochastic approach naturally reproduces the inverse correlation between Ag concentration and heterogeneity in Ab affinities (Figures S2G and S2H) observed in early experiments (Eisen and Siskind, 1964).

For the three immunization schemes with antigen variants, Ag concentration is again a very important variable (Figure 2). If the Ag concentration is too low, most GCs collapse as expected. However, there is a curious decline in GC survival and Ab breadth if the Ag concentration is too high for immunization schemes II and III. During AM after immunizing with a high dose of WT Ag, many B cells survive easily and the GC reaction draws to an end quickly. Therefore, these B cells are largely low-affinity clones that have not accumulated mutations that enhance contacts with the conserved residues of the epitope. So, upon administering either a cocktail of the two Ag variants or just one variant, these B cells have a small chance of binding sufficiently strongly with the mutants and surviving, and so GCs collapse despite the abundance of Ag. The few Abs produced do not develop breadth as the large number of mutations required to confer breadth do not evolve (see examples in Figure S3).

Hereon, for each immunization scheme, we show results for the Ag concentration (listed in Table 1) that yields Abs with a

Table 1. Properties of Antibody Responses Produced by Various Immunization Schemes

Scheme	%surv	Breadth	h_c	h_v	C_{tot}
WT only (t_{max} = 80)					
Ab feedback	54%	0.6%	0.45	0.39	0.3
peers only	79%	0.7%	0.49	0.43	0.5
(I) WT+v1+v2 (t_{max} = 240)					
See 1 Ag; Ab feedback	1%	11%	0.72	0.29	0.6
peers only	1%	2%	0.52	0.22	1.0
See all Ag; Ab feedback	1%	5%	0.84	0.70	0.3
peers only	3%	3%	0.89	0.83	0.5
(II) WT|v1+v2 (t_{max} = 80 + 160 = 240)					
See 1 Ag; Ab feedback	80%	75%	1.21	0.16	0.36
peers only	10%	35%	0.73	0.16	1.0
See both Ag; Ab feedback	31%	33%	1.07	0.37	0.3
peers only	47%	42%	1.22	0.41	0.5
(II) WT|v1|v2 (t_{max} = 80 × 3 = 240)					
Ab feedback	43%	79%	1.38	0.22	0.33
peers only	69%	83%	1.64	0.24	0.55

%surv: percentage of seeded GCs that produce antibodies efficiently; Breadth: defined in text; h_c (h_v): the average strength of interactions with conserved (variable) residues of the epitope—large values of h_c indicate focusing on the conserved residues of the epitope; C_{tot}: antigen concentration.

near optimal breadth (peak of red curves in Figure 2). In scheme III, the chosen concentration is slightly higher to ensure high Ab production.

Immunizing with a Cocktail of WT Ag and Two Variants Fails to Elicit an Effective Response

Figure 3A shows in silico results for the distribution of the breadth of coverage (for the Seeman panel) of Abs produced using immunization scheme I (cocktail of WT+v1+v2). Ag concentration is fixed to yield the greatest breadth, but two more variables could be important: during selection in the light zone, does a B cell-FDC encounter involve one or all Ag variants? Is "Ab feedback" important during AM? For this immunization scheme, in most scenarios, just a few percent of GCs survive (Table 1); i.e., Ab titers are predicted to be low. To see why, consider first the situation where B cells interact with only one Ag variant during each encounter with FDCs. B cells that bind moderately strongly to one of the three variants seed the GC, and they do not have any strong interactions with the conserved residues of the epitope yet. Now consider a B cell that is selected by a particular Ag variant in an early round, then mutates, and returns to the light zone to encounter a different variant. Without even moderately strong contact with the conserved residues, the probability that such a B cell is cross-reactive to the new variant is small. Thus, apoptosis is the most likely outcome, leading to collapse of the GC. For the rare GCs that do survive, there is evolution of interactions with the conserved residues and dimunition of interactions with variable loops during AM, and this confers some breadth (relative to immunization with WT Ag alone, see Table 1).

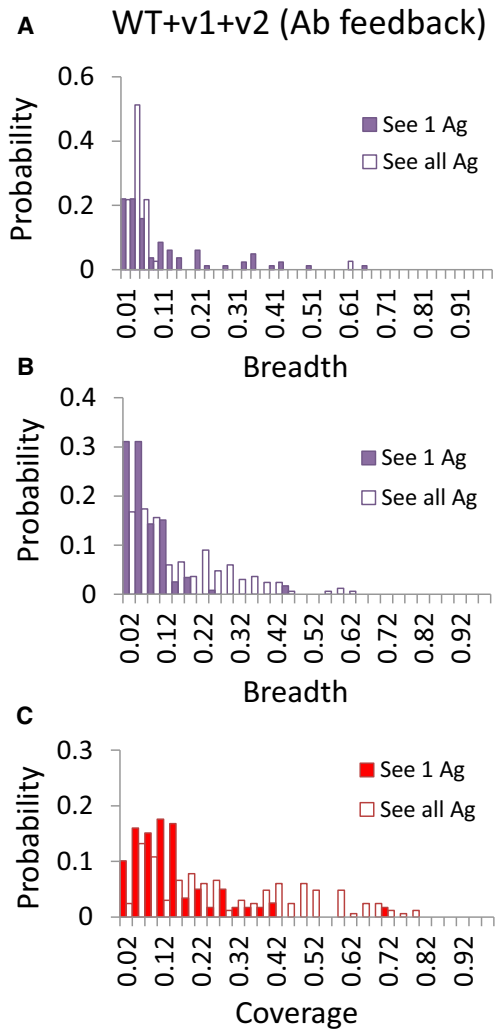

Figure 3. Distribution of Breadth of Individual Antibodies and Their Total Coverage for Surviving GCs in Scheme I—WT+v1+v2

(A and B) Histograms of breadth for having 11 (A) or 4 (B) non-overlapping mutations in the two variants. Histograms are obtained as a distribution for all the surviving GCs.

(C) Histograms of coverage for surviving GCs under the same conditions as in (B). The coverage is defined as a sum of non-overlapping specificities. Results are shown for the cases of "see 1 Ag" (filled bars) and "see all Ag" (unfilled bars), with Ab feedback.

See also Figure S4.

If B cells interact with all Ag variants during each encounter with FDCs, and the Ag concentration is chosen to be the one that confers optimal breadth, the percentage of surviving GCs and the distribution of breadth is not very different compared to the case where only one Ag variant is encountered at a time (Figure 3A). However, importantly, the optimal concentration is lower when B cells can interact with all Ag variants. If the Ag concentrations were made the same as when B cells interact with one Ag at a time, then most GCs would survive when all Ag variants are simultaneously encountered (Figure S4B). This is because, in this case, B cells that bind sufficiently strongly to

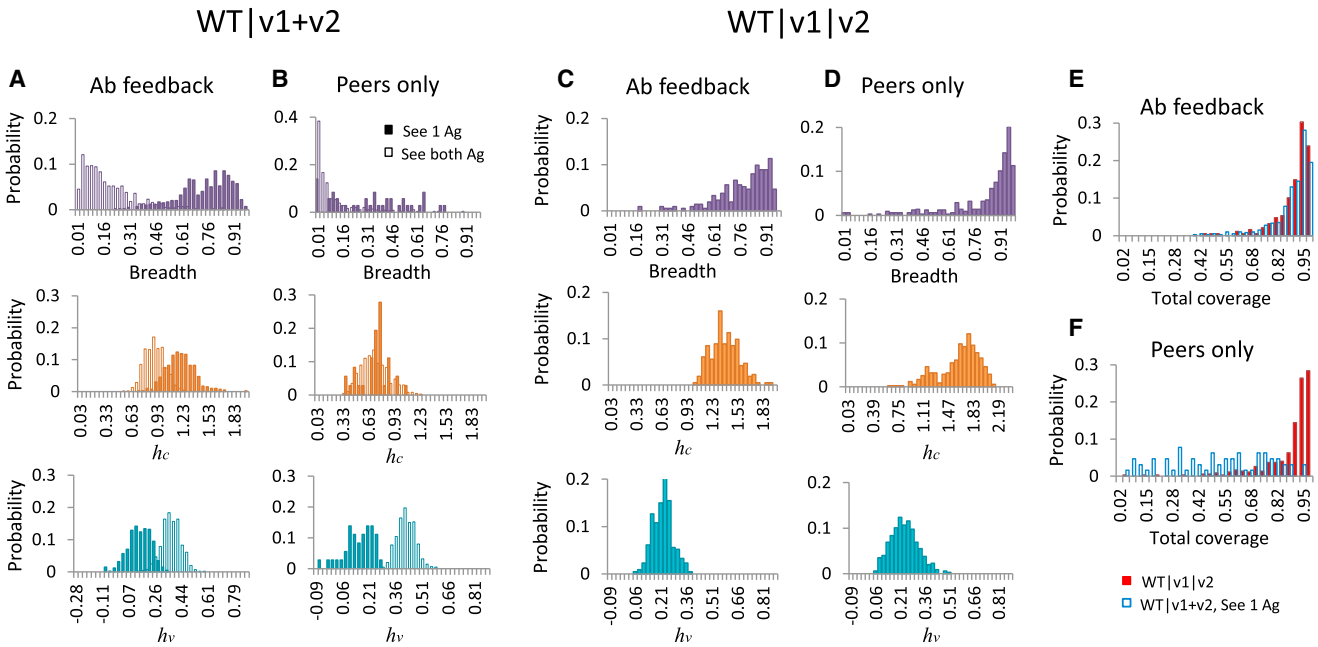

Figure 4. Comparison of Statistics for Surviving GCs in Scheme II—WT|v1+v2 and Scheme III—WT|v1|v2

(A–F) Shown are histograms for breadth, mean interaction strength with conserved residues (h_c) and with variable residues (h_v) (A–D), and for total coverage (E and F) via a polyclonal response. Results are shown for "Ab feedback" (A, C, and E) and "peers only" (B, D, and F) scenarios. For scheme II (A and B), cases of "see 1 Ag" (filled bars) and "see both Ag" (unfilled bars) are shown. Total coverage (E and F) is presented for scheme III (WT|v1|v2) by red filled bars and for scheme II (WT|v1+v2, see 1 Ag) by blue unfilled bars. See also Figure S5.

any one Ag variant can progress through AM. As a consequence, the generated Abs are likely to be strain specific. Thus, if Ag is displayed homogeneously on FDCs, for immunization scheme I, optimal conditions for inducing Abs efficiently at high titers would not induce bnAbs. The lower Ag concentration required for optimal breadth results in the survival of only a relatively low fraction of GCs (Figure 3A).

We also carried out calculations where the Ag variants differ from each other by only four non-overlapping mutations. When all variants are simultaneously encountered in each interaction with FDCs and Ab feedback is turned on, comparing results for this case (Figure 3B) with that when the variants differ by 11 mutations (Figure 3A), we find that a much higher fraction (10% versus 1%) of GCs succeed in producing Abs (Figure S4D). This is because the Ags vary less from each other, and so the chance of a B cell being cross-reactive to variants in early stages of AM is higher, thus increasing the probability of it being positively selected. The breadth of the Abs produced is not large because many variable residues that are unmutated in the Ag variants are mutated in the test panel sequences, and strain specific Abs are likely to be produced as all Ag variants on FDCs are simultaneously encountered. This is why the total coverage (Figure 3C), defined as the breadth of coverage offered by the polyclonal response from all the Abs, is higher than the average breadth of coverage of individual Abs (Figure 3B). Results for the case where only one Ag variant is encountered at a time on FDCs are shown in Figures 3B and 3C (filled bars), and for no Ab feedback see Table 1.

In our in silico studies of this immunization scheme, we did not find any conditions that result in bnAbs with high probability (Figure S4). This is because B cell evolution during AM is made difficult by the potentially conflicting selective pressures imposed by Ag variants simultaneously displayed on FDCs. We term this phenomenon, *frustrated AM*. The degree to which AM is frustrated is controlled by a complex interplay between Ag concentration, heterogeneity of Ag display on the FDCs, the number of mutations that separate the Ag variants, and the extent to which Ab feedback is important.

Immunizing with WT Ag First and then a Cocktail of the Two Variants Yields Abs with Significant Breadth in Special Circumstances

Consider first the situation in which there is no Ab feedback and only one Ag variant is encountered at a time on FDCs (Figure 4B filled bars). In the first period of AM induced by the WT Ag, moderately strong contacts with the conserved residues of the epitope can evolve. During AM following immunization with the cocktail, individual B cells have equal chance of encountering either Ag variant during selection. Since the two variants have non-overlapping mutated residues, beneficial BCR mutations for one strain are deleterious for the other. Maturing B cell lineages are frustrated in satisfying these conflicting requirements for selection in successive rounds, but less so than in scheme I because moderately strong interactions with the conserved residues have evolved during AM driven by the WT Ag prime, resulting in some cross-reactivity. Therefore, a greater fraction (~10%) of GCs survive compared to scheme I. Since a relatively high Ag

concentration is required for GC survival in this case (Figure 2A right panel blue curve), B cells can expand readily and GCRs terminate quickly. Short maturation times limit the average breadth (~35%, Figure 2A right, red curve), but Abs with large breadth do evolve with low probability.

If there is Ab feedback, lower Ag concentrations still allow GCs to mature successfully. This is because Abs produced in previous rounds of AM often have lower affinities for the encountered Ag than the best clones produced during the current round of mutation and selection. This confers a competitive advantage to these best B cell clones because they are not just competing with each other, but also with the weaker affinity Abs ("Simulation Methods" in Extended Experimental Procedures). Also, the Abs compete effectively with unfavorable mutant cells that may emerge and be stochastically selected only to be extinguished in a future round of mutation-selection. Lowering Ag concentration diminishes the probability of selection in each round, thus allowing AM to proceed for a longer time before all the Ag on FDCs is internalized. This allows mutations that confer breadth to accumulate. This balance of lowering frustration through Ab feedback and increasing frustration by reducing Ag concentration results in a very high survival rate for GCs and considerable breadth in the Ab response (Figure 2A left, Figure 4A filled bars).

If multiple Ags are encountered during each interaction with FDCs, the outcome is different (Figures 4A and 4B, unfilled bars). Since a choice of being selected by the same variant (rather than a randomly chosen one of the two) is always available in successive rounds of AM, the frustration is low. In most cases, we find that B cells are selected by one of the variants repeatedly, and so strain-specific Abs are likely to evolve (Table 1). Furthermore, access to both Ag variants allows B cells to multiply successfully in the GC and quickly consume all the Ag on FDCs. The duration of AM is short, so mutations that confer breadth evolve rarely, and the average breadth is no more than 40%, regardless of the extent of Ab feedback (Table 1). For this optimal breadth to develop, the antigen concentrations must be much lower than when only one Ag variant is seen during each B cell-FDC encounter (Figure 2B versus 2A).

Our results suggest that this immunization scheme has the potential to produce bnAbs (~75% breadth) with high probability if B cells encounter one Ag variant at a time on FDCs and all Abs produced in previous rounds migrate through ongoing GCs. Rather than the extreme situations of full Ab feedback or none at all, there is some middle ground, and also most likely, B cells encounter one FDC Ag variant in some rounds of selection and all variants during others. Thus, our results suggest that, depending upon circumstances, this immunization scheme produces Abs efficiently with a probability between 10%–80%, and with average breadths ranging from 30% to 80% (Table 1). This scheme may be analogous to what ensues in patients who develop bnAbs upon natural infection as they are first exposed to the infecting strain, which then diversifies. However, the sensitivity of our results to varying conditions suggest that it may be quite difficult to induce bnAbs consistently in diverse patients using this immunization scheme. This is because the conditions noted above are likely to vary between and within individuals.

Sequential Immunization with Antigen Variants Leads to Efficient Induction of an Antibody Response with Broad Specificity

Sequential immunization with the three Ag variants temporally separates the mutually conflicting selective driving forces imposed by multiple variants. Confounding effects associated with whether one or multiple types of Ags participate in each B cell-FDC encounter in the GC are also obviated.

Consider first the situation where there is no Ab feedback (Figure 4D). Maturation against the WT Ag results in some strong interactions with the conserved residues. When AM ensues with the first variant, two main types of lineages evolve in the simulations (Figure S5). Both types of lineages tend to reduce interactions with the residues that are mutated in the first variant Ag. But, in one type of lineage, interactions with the unmutated variable residues in the first variant (which are mutated in the second variant) are enhanced; in the other type of lineage, these interactions do not change much. When the second variant with non-overlapping mutations is introduced, the latter lineages have a good chance of outcompeting the former ones during AM. This is because clones that did not increase their footprint on the variable residues that are now mutated in the second variant can simply reduce interactions with these residues, and focus strongly only on the conserved residues of the epitope. This is why Abs produced in scheme III exhibit a narrow distribution of very large breadth (Figure 4D top panel) rather than a broad distribution of Abs with moderate breadth seen in the analogous situation using scheme II (Figure 4B top panel, filled bars). In scheme II, lineages specific for one or the other variant strain have a higher chance of survival. In scheme III, Abs that focus contacts with the conserved residues of the epitope and minimize interactions with all the variable residues are more likely to emerge (Figures 4B and 4D, middle panels).

Comparing "Ab feedback" (Figure 4C) and "peers only" scenarios (Figure 4D) in scheme III, we see that Ab feedback leads to narrower distributions of Abs with large breadth, due to the same effects of Ab feedback noted for scheme II. As shown in Figures 4E and 4F, the distributions of total coverage for Abs produced by schemes II and III are very close when there is Ab feedback (Figure 4E), and the average values are both as high as 90%. If there is no Ab feedback (Figure 4F), however, scheme III gives a similar broad coverage (89%), whereas scheme II yields a moderate coverage (51%) even with polyclonal responses. So, scheme III is predicted to be more robust to many varying conditions.

Experiments in Mice with a Model System Show that Antibodies that Focus on the Conserved Residues Emerge upon Sequential Immunization, but Not upon Immunization with a Cocktail

Our calculations predict that, compared to the other immunization schemes we studied, truly cross-reactive Abs that focus contacts on the conserved residues of the epitope with a small footprint outside are most likely to emerge robustly upon sequential immunization with Ag variants. Immunization with a cocktail of Ags is predicted to result in a significantly worse outcome compared to sequential immunization. We

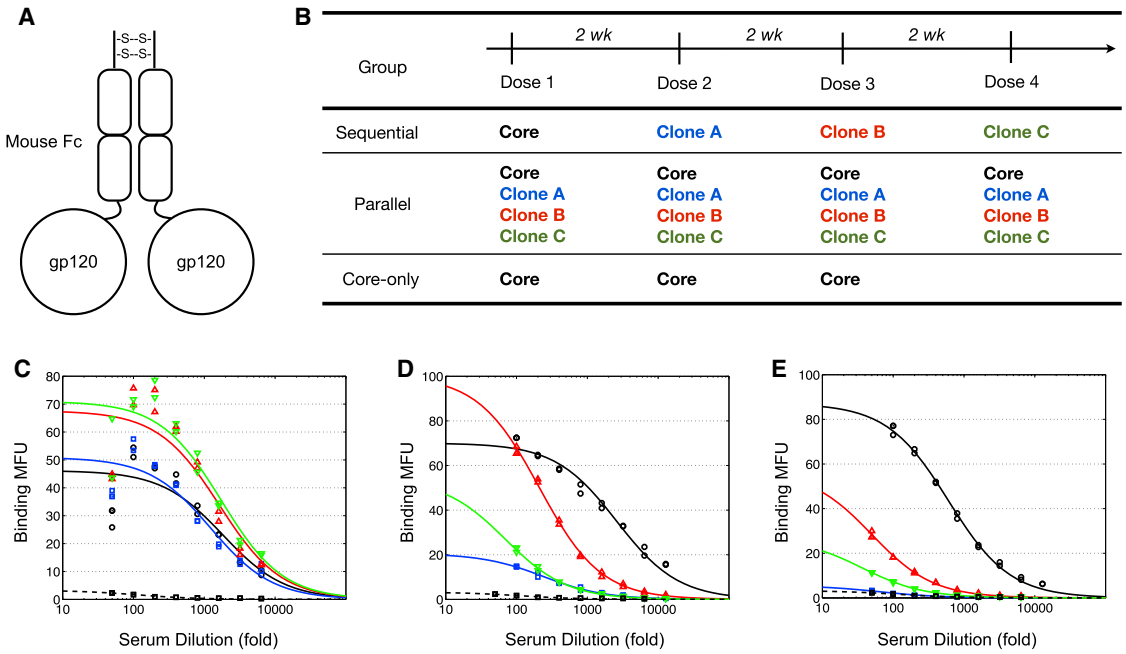

Figure 5. Immunization of Mice with Variant Immunogens

(A) Schematic of an Fc-gp120 immunogen.

(B) Immunization groups and dosing schedule for mouse experiment.

(C–E) Serum titrations (day 48) of a representative mouse from each group—(C) sequential, (D) parallel, (E) core-only—on yeast displaying stripped core (black), clone A (blue), clone B (red), or clone C (green). Each plot also includes serum from an unimmunized mouse binding to yeast displaying clone C (black dashed). Binding data are fit to a monovalent binding isotherm of the form $y = y_{max}\, dil^{-1}/(dil^{-1} + K_A^{-1})$ where "dil" is the serum dilution and y is the binding signal in MFU. Discussion of the fitted parameters can be found in the supplemental material.

See also Figure S6 and Table S1.

note previous immunization studies that have suggested the advantages of sequential immunization of HIV Env in generating cross-reactive Abs, in further agreement with our computational results (Malherbe et al., 2011; Pissani et al., 2012). Here, we tested our predictions comparing sequential immunization and cocktails in mouse studies using precisely engineered Ag variants. It is important to note that the variant Ags we have engineered are gp120 monomers of Env, not trimers. Thus, they cannot be expected to produce bnAbs that neutralize virus particles with intact trimeric spikes. The goal of our experiments was to precisely test whether cross-reactive Abs that focus on the conserved residues of an epitope (CD4bs) are more likely to develop upon sequential immunization, compared to administration of a cocktail of the same immunogens, as per our in silico predictions.

As described in Extended Experimental Procedures, we engineered variants of a minimized gp120 core protein immunogen (the "stripped core") that incorporate diversification at 43 surface residues outside the CD4bs, while retaining binding affinity to the VRC01 bnAb (Table S1, Figure S6). These immunogens are designed to present biochemically novel residues outside the CD4bs such that only the desired CD4bs epitope is conserved across all the immunogens. We used four engineered variants (including stripped core) that fit these criteria. Our in silico results should hold irrespective of whether three or four variants are used.

BALB/c mice were immunized intranasally with HEK293-produced immunogens fused to mouse Fc (Figure 5A) with a CpG oligonucleotide adjuvant, following protocols described elsewhere (Ye et al., 2011). Immunogens were administered every 2 weeks at a total protein dose of 50 pmol. Animals were divided into three groups (Figure 5B). The "Sequential" group of four mice was immunized sequentially with each of the four Ag variants. The "Parallel" group of four mice received a cocktail of all four variants at each administration. The "core-only" group of two mice was given three doses of the same stripped core immunogen. Serum was collected every week.

Serum binding to the Ag variants was assayed by flow cytometry of yeast displaying each of the four variants. Representative curves for each of the three immunization groups are shown in Figures 5C–5E. Sequentially immunized mice exhibit similar binding to each of the four Ag variants, consistent with serum that recognizes and focuses contacts with a shared epitope presented on all variants (Figure 5C). Mice immunized with a cocktail of four variants show a broader spread of binding affinities, consistent with dominant serum specificities for some variants but not others (Figure 5D). In the mouse represented, for example, it appears that the serum recognizes the epitope on stripped core that is not present on clones A or C. Serum from mice immunized only with stripped core bind strongly to stripped core but not to the other immunogens, consistent with our immunogen design objective that the four variants not share common

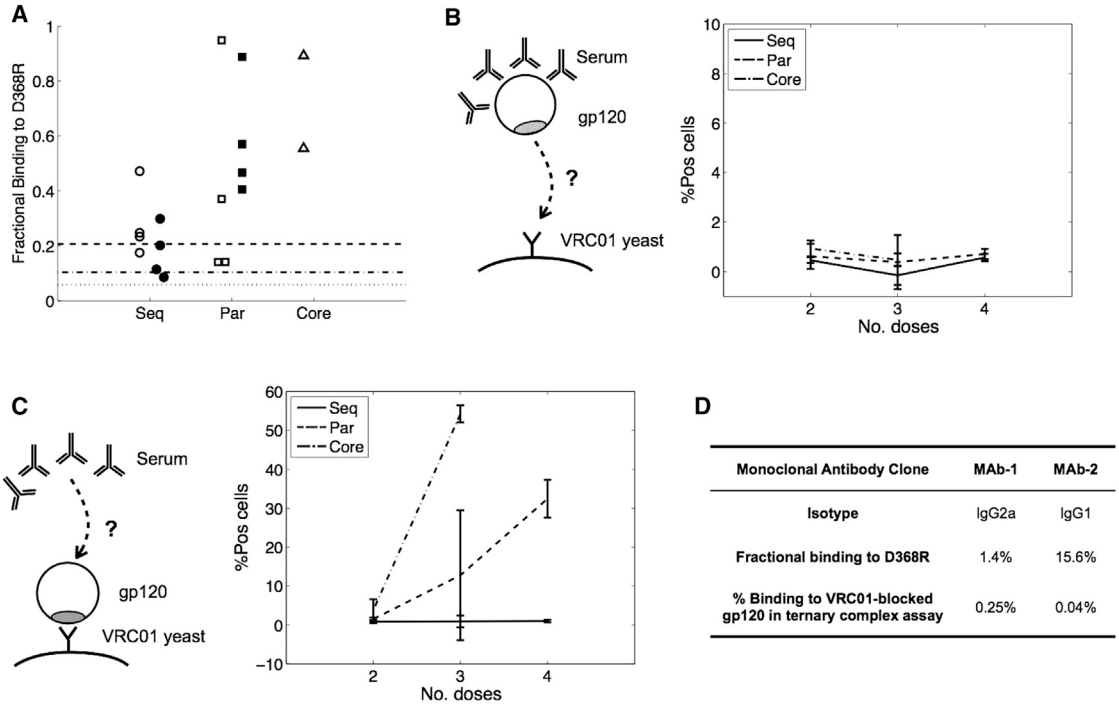

Monoclonal Antibody Clone	MAb-1	MAb-2
Isotype	IgG2a	IgG1
Fractional binding to D368R	1.4%	15.6%
% Binding to VRC01-blocked gp120 in ternary complex assay	0.25%	0.04%

Figure 6. Determination of Serum Specificity for the CD4 Binding Site

(A) Fractional binding to D368R mutant versus stripped core of serum from each group after three (open markers) and four (filled markers) immunizations. The fractional binding to D368R for antibody VRC01 at various concentrations is shown as lines: 0.21 at 93 nM (dashed line), 0.10 at 75 nM (dash-dotted line), and 0.06 at 8.2 nM (dotted line).

(B) Schematic and data from ternary complex assay in which gp120 (CD4bs shown in gray) is pre-incubated with serum then added to VRC01 yeast. The formation of a ternary complex is only possible if VRC01 is able to bind to its epitope on gp120 after serum has bound. The figure shows the percentage of yeast cells positive for mouse serum from each immunization group—sequential (solid line), parallel (dashed line), core-only (dash-dotted line)—for various time points (mean ± SD).

(C) Schematic and data from ternary complex assay in which gp120 is pre-loaded onto VRC01 yeast then incubated with serum. The formation of a ternary complex is only possible if serum antibodies are able to bind to their epitope(s) after VRC01 has bound. The figure shows the percentage of yeast cells positive for mouse serum from each immunization group as above.

(D) Analysis of two monoclonal antibodies from a sequentially immunized mouse: fractional binding to D368R versus stripped core gp120 was assayed with 10 nM monoclonal antibody (analogous to 6A); percentage binding in the ternary complex assay (analogous to 6C), in which gp120 is pre-bound to VRC01 yeast.

surface residues outside the CD4bs (Figure 5E), like the non-overlapping mutations in Ag variants in our calculations.

Serum specificity for the CD4bs was determined in two ways. First, we measured the binding of serum to the stripped core mutant D368R, which is known to disrupt the binding of several CD4bs-directed Abs (Thali et al., 1992). Serum samples collected after the third and fourth immunizations were incubated at a 1:100 dilution with yeast displaying either stripped core or the D368R mutant (Figure 6A). For mice from the sequential immunization group, the fractional binding of serum to D368R was similar to that of VRC01 at saturating concentrations. Of the mice that were immunized with a cocktail of all four immunogens, three are very sensitive to D368R after three immunizations but appear to lose this specificity by the fourth administration.

A second assay used to determine specificity was to evaluate the simultaneous binding of VRC01 and serum antibodies to gp120 (Experimental Procedures). The assay was performed first by pre-incubating the gp120 with mouse serum before introducing VRC01-displaying yeast (Figure 6B). If serum antibodies compete with VRC01 for its binding site, the gp120-serum complex will not bind to the yeast. No binding signal was observed for any of the serum samples, suggesting that all contained some fraction of VRC01-competitive antibodies. This result is consistent with the D368R gp120 binding results discussed above.

The same assay was then performed by pre-incubating gp120 with VRC01 yeast before introducing the serum (Figure 6C) to determine whether the serum contains any specificity other than to the CD4bs. Note that due to plasmid loss in yeast during culture, ~60% positive cells is the maximum observable signal in the assay. Mice immunized with just stripped core (53%, 56%) or with a cocktail of four Ags (mean = 32% ± 5%) developed antibodies that bind to other epitopes on gp120. However, mice immunized sequentially did not (mean = 1.0% ± 0.3%). These experiments suggest that sequential immunization with Ag variants elicited a serum response that was VRC01-competitive and entirely focused on the conserved residues targeted by the VRC01 Ab. Mice that were exposed to a cocktail of the variants generated some VRC01-competitive antibodies, but also Abs that targeted non-conserved residues on a single immunogen, i.e., were not cross-reactive. In other words, only sequential

immunization robustly elicited a response that is focused on the conserved residues of the desired epitope. These findings are in harmony with our in silico results.

To establish that individual CD4bs-competitive antibodies were generated by sequential immunization, hybridomas were generated by splenotypic fusion from a mouse immunized using this protocol. Two distinct gp120-binding monoclonal antibodies were isolated (for sequences, see Extended Experimental Procedures). The antibodies both targeted the CD4bs epitope, as both were disrupted by the D368R mutation (at 10 nM antibody, fractional binding to D368R versus stripped core gp120 of 1.4% and 15.6%) and neither was able to bind to stripped core that had been pre-blocked with VRC01 (Figure 6D). These data make clear that the monoclonal antibodies are indeed focused on the CD4bs upon sequential immunization with the variant antigens.

DISCUSSION

The induction of bnAbs against highly mutable pathogens, such as HIV and influenza, will require immunization with Ag variants. Rational design of immunogens and efficient immunization protocols that elicit bnAbs requires mechanistic understanding of a basic problem in immunobiology: viz., how AM occurs in the presence of variant Ags. Our studies of AM in this setting have revealed new concepts, suggested new avenues for experimental and theoretical research, and have practical value. An important concept that emerges is that, when multiple Ag variants are used as immunogens, they can present conflicting selection forces during AM which frustrates the evolution of Abs. This phenomenon is most acutely manifested upon immunization with a cocktail of Ag variants. In this case, a B cell of a particular lineage that is selected in one round by a particular Ag variant is likely, after the next round of mutation, to encounter a different Ag variant on FDCs. This B cell is unlikely to be positively selected in this encounter, thus ending the evolution of a potentially favorable B cell lineage. The degree to which AM is frustrated is determined by a complex interplay of effects dependent on Ag concentration, how heterogeneously Ag variants are displayed on FDCs, the number of mutations that separate the Ag variants, and the extent to which previously generated Abs migrate through ongoing GCs. Our results provide empirical evidence that these parameters can be tuned to achieve an optimal level of frustration. Too much frustration prevents GC reactions from evolving favorable mutations that confer breadth. Too low a level of frustration (the extreme case being immunization with one Ag) results in the development of strain-specific antibodies. An avenue for future theoretical research is to define a quantitative metric of frustration that describes precisely how the degree of frustration depends on the pertinent variables. The metric of frustration could then be optimized to design effective immunization protocols.

Our in silico results suggest that if one primes with the WT Ag, and then boosts with a cocktail of variants, bnAbs can emerge but only if some special conditions hold. Such a scenario may have been the driver of bnAb production in naturally infected patients because this immunization strategy mimics natural infection with one strain and subsequent viral diversification. However, our results show that deviations from these special conditions make the evolution of bnAbs unlikely in this setting (Table 1). This suggests that potent bnAbs evolve during natural infection only when special conditions are met, which happens rarely, and thus take a long time to emerge by chance. Controlling immunization protocols precisely to satisfy special conditions in every vaccinated individual seems difficult. Furthermore, even if the conditions were set to perfectly mimic a situation that resulted in the evolution of bnAbs upon natural infection, the outcome may not be favorable because Darwinian evolution is inherently stochastic and cannot be replicated exactly. So, although it is important to understand how bnAbs are produced during natural infection, mimicking these conditions may not be an efficient way to induce bnAbs by vaccination.

We find that when Ag variants are administered sequentially, bnAbs can develop with relatively high probability over a wider range of conditions than if other strategies are deployed (Table 1, and Figures 2, 3, and 4). In this case, the conflicting selection forces due to the variant Ags are temporally separated. This can lead to successful evolution of multiple B cell lineages that first develop moderate interactions with the conserved residues of the epitope and then progressively acquire mutations that evade contacts with one set of variable residues and then another. Evolution of a set of possible clones which have a chance at maturing into bnAbs after AM against the first variant makes success more likely as all of them are unlikely to go extinct during stochastic mutation and selection upon immunizing with the second variant. Our in silico results predict that this immunization strategy is superior to immunization with a cocktail of the same set of variants, and our model experiments in mice support this prediction.

Sequential immunization with Ag variants that share a single epitope to induce B cells specific for the common epitope has been tried with linear peptide epitopes derived from HIV gp41, though the resulting Abs were non-neutralizing (Guenaga et al., 2011; Correia et al., 2010). Past work also emphasizes the importance of masking irrelevant epitopes, but by itself, this strategy is insufficient for successful vaccination (Pantophlet et al., 2003; Selvarajah et al., 2005). Our in silico and in vivo studies suggest that precisely engineered variant intact virus spike immunogens administered in a sequential fashion under appropriate conditions may offer the best opportunities for induction of bnAbs against HIV-1 and other highly mutable pathogens.

EXPERIMENTAL PROCEDURES

In Silico Model

The probability of a B cell internalizing antigen is given by:

$$P_a^i = \frac{\sum_{j=1}^{n_A} C_j e^{(E_{ij}-E_a)/k_B T}}{1+\sum_{j=1}^{n_A} C_j e^{(E_{ij}-E_a)/k_B T}}. \quad (1)$$

Here C_j is the concentration of Ag of type j presented on the FDCs. The sum over the Ag index j runs through n_A distinct types of Ags that B cell i could potentially interact with simultaneously during an encounter with a FDC bearing multiple Ag variants.

The probability of a B cell to succeed in receiving T cell help is given by:

$$P_{Th}^{i} = \frac{\sum_{j=1}^{n_A} e^{E_{ij}/k_B T}}{\sum_{j=1}^{n_A} e^{E_{ij}/k_B T} + C_{tot}^{-1} \left\langle \sum_{j'=1}^{n_A} e^{E_{i'j'}/k_B T} \right\rangle_{i'(\neq i)}}, \quad (2)$$

where $\langle \sum_{j'=1}^{n_A} e^{E_{i'j'}/k_B T} \rangle_{i'(\neq i)}$ is the average probability of internalizing Ag of all the other B cells present in the GC. $C_{tot} = \sum_{j=1}^{n_A} C_j$ is the total Ag concentration, and the dependence on this variable accounts for the observation that the number of activated T helper cells increases with Ag dose, thus making it more likely that B cells receive T cell help.

Binding Assay to Determine Competitiveness with VRCO1

Yeast displaying the scFv of VRC01 was incubated with soluble stripped core gp120 and an excess of mouse antiserum. The formation of a ternary complex—a sandwich of VRC01, gp120, and mouse serum—was detected as the presence of mouse antibodies on yeast by flow cytometry (% positive cells). The experiment was done in two ways as described in text.

See Extended Experimental Procedures for additional information.

SUPPLEMENTAL INFORMATION

Supplemental Information includes Extended Experimental Procedures, six figures, and one table and can be found with this article online at http://dx.doi.org/10.1016/j.cell.2015.01.027.

AUTHOR CONTRIBUTIONS

S.W., A.K.C., M.K., and D.R.B. conceived and designed in silico studies; S.W., A.K.C., M.K. analyzed in silico data; S.W. performed in silico studies; J.M.F., D.J.I., M.H., K.D.W. designed experiments and J.M.F., K.D.W. analyzed data; J.M.F. performed experiments; B.K. helped engineer Ag variants; A.K.C., S.W., M.K., J.M.F., K.D.W., D.R.B., H.N.E. wrote paper.

ACKNOWLEDGMENTS

Financial support provided by the Ragon Institute of MGH, MIT, and Harvard (AKC, SW, MK, KDW, JMF) and the International AIDS Vaccine Initiative (IAVI) through the Neutralizing Antibody Consortium SFP1849 (DRB); NIH grants R01 AI033292 (DRB), and Center for HIV/AIDS Vaccine Immunology and Immunogen Discovery grant UM1AI100663 (DRB, AKC). We are grateful to Kevin Kaczorowski and Dariusz Murakowski for helpful discussions and comments.

Received: July 2, 2014
Revised: October 3, 2014
Accepted: December 19, 2014
Published: February 5, 2015

REFERENCES

Allen, C.D.C., Okada, T., Tang, H.L., and Cyster, J.G. (2007). Imaging of germinal center selection events during affinity maturation. Science *315*, 528–531.

Batista, F.D., and Neuberger, M.S. (1998). Affinity dependence of the B cell response to antigen: a threshold, a ceiling, and the importance of off-rate. Immunity *8*, 751–759.

Baumjohann, D., Preite, S., Reboldi, A., Ronchi, F., Ansel, K.M., Lanzavecchia, A., and Sallusto, F. (2013). Persistent antigen and germinal center B cells sustain T follicular helper cell responses and phenotype. Immunity *38*, 596–605.

Berek, C., and Milstein, C. (1987). Mutation drift and repertoire shift in the maturation of the immune response. Immunol. Rev. *96*, 23–41.

Berek, C., Berger, A., and Apel, M. (1991). Maturation of the immune response in germinal centers. Cell *67*, 1121–1129.

Burton, D.R., Ahmed, R., Barouch, D.H., Butera, S.T., Crotty, S., Godzik, A., Kaufmann, D.E., McElrath, M.J., Nussenzweig, M.C., Pulendran, B., et al. (2012). A blueprint for HIV vaccine discovery. Cell Host Microbe *12*, 396–407.

Correia, B.E., Ban, Y.E., Holmes, M.A., Xu, H., Ellingson, K., Kraft, Z., Carrico, C., Boni, E., Sather, D.N., Zenobia, C., et al. (2010). Computational design of epitope-scaffolds allows induction of antibodies specific for a poorly immunogenic HIV vaccine epitope. Structure *18*, 1116–1126.

Deem, M.W., and Lee, H.Y. (2003). Sequence space localization in the immune system response to vaccination and disease. Phys. Rev. Lett. *91*, 068101.

Eisen, H.N., and Siskind, G.W. (1964). Variations in affinities of antibodies during the immune response. Biochemistry *3*, 996–1008.

Gao, F., Bonsignori, M., Liao, H.X., Kumar, A., Xia, S.M., Lu, X., Cai, F., Hwang, K.K., Song, H., Zhou, T., et al. (2014). Cooperation of B cell lineages in induction of HIV-1-broadly neutralizing antibodies. Cell *158*, 481–491.

Goidl, E.A., Paul, W.E., Siskind, G.W., and Benacerraf, B. (1968). The effect of antigen dose and time after immunization on the amount and affinity of anti-hapten antibody. J. Immunol. *100*, 371–375.

Guenaga, J., Dosenovic, P., Ofek, G., Baker, D., Schief, W.R., Kwong, P.D., Karlsson Hedestam, G.B., and Wyatt, R.T. (2011). Heterologous epitope-scaffold prime:boosting immuno-focuses B cell responses to the HIV-1 gp41 2F5 neutralization determinant. PLoS ONE *6*, e16074.

Jacob, J., Kassir, R., and Kelsoe, G. (1991). In situ studies of the primary immune response to (4-hydroxy-3-nitrophenyl)acetyl. I. The architecture and dynamics of responding cell populations. J. Exp. Med. *173*, 1165–1175.

Julien, J.-P., Cupo, A., Sok, D., Stanfield, R.L., Lyumkis, D., Deller, M.C., Klasse, P.J., Burton, D.R., Sanders, R.W., Moore, J.P., et al. (2013). Crystal structure of a soluble cleaved HIV-1 envelope trimer. Science *342*, 1477–1483.

Källberg, E., Jainandunsing, S., Gray, D., and Leanderson, T. (1996). Somatic mutation of immunoglobulin V genes in vitro. Science *271*, 1285–1289.

Kelsoe, G. (1996). The germinal center: a crucible for lymphocyte selection. Semin. Immunol. *8*, 179–184.

Kepler, T.B., and Perelson, A.S. (1993). Somatic hypermutation in B cells: an optimal control treatment. J. Theor. Biol. *164*, 37–64.

Kepler, T.B., Munshaw, S., Wiehe, K., Zhang, R., Yu, J.S., Woods, C.W., Denny, T.N., Tomaras, G.D., Alam, S.M., Moody, M.A., et al. (2014). Reconstructing a B-cell clonal lineage. II. mutation, selection, and affinity maturation. Front. Immunol. *5*, 170.

Keşmir, C., and De Boer, R.J. (2003). A spatial model of germinal center reactions: cellular adhesion based sorting of B cells results in efficient affinity maturation. J. Theor. Biol. *222*, 9–22.

Klein, F., Diskin, R., Scheid, J.F., Gaebler, C., Mouquet, H., Georgiev, I.S., Pancera, M., Zhou, T., Incesu, R.-B., Fu, B.Z., et al. (2013). Somatic mutations of the immunoglobulin framework are generally required for broad and potent HIV-1 neutralization. Cell *153*, 126–138.

Kocks, C., and Rajewsky, K. (1988). Stepwise intraclonal maturation of antibody affinity through somatic hypermutation. Proc. Natl. Acad. Sci. USA *85*, 8206–8210.

Kroese, F.G.M., Wubbena, A.S., Seijen, H.G., and Nieuwenhuis, P. (1987). Germinal centers develop oligoclonally. Eur. J. Immunol. *17*, 1069–1072.

Kwong, P.D., Doyle, M.L., Casper, D.J., Cicala, C., Leavitt, S.A., Majeed, S., Steenbeke, T.D., Venturi, M., Chaiken, I., Fung, M., et al. (2002). HIV-1 evades antibody-mediated neutralization through conformational masking of receptor-binding sites. Nature *420*, 678–682.

Kwong, P.D., Mascola, J.R., and Nabel, G.J. (2013). Broadly neutralizing antibodies and the search for an HIV-1 vaccine: the end of the beginning. Nat. Rev. Immunol. *13*, 693–701.

Liao, H.-X., Lynch, R., Zhou, T., Gao, F., Alam, S.M., Boyd, S.D., Fire, A.Z., Roskin, K.M., Schramm, C.A., Zhang, Z., et al.; NISC Comparative Sequencing Program (2013). Co-evolution of a broadly neutralizing HIV-1 antibody and founder virus. Nature *496*, 469–476.

Lyumkis, D., Julien, J.P., de Val, N., Cupo, A., Potter, C.S., Klasse, P.J., Burton, D.R., Sanders, R.W., Moore, J.P., Carragher, B., et al. (2013). Cryo-EM structure of a fully glycosylated soluble cleaved HIV-1 envelope trimer. Science *342*, 1484–1490.

Malherbe, D.C., Doria-Rose, N.A., Misher, L., Beckett, T., Puryear, W.B., Schuman, J.T., Kraft, Z., O'Malley, J., Mori, M., Srivastava, I., et al. (2011). Sequential immunization with a subtype B HIV-1 envelope quasispecies partially mimics the in vivo development of neutralizing antibodies. J. Virol. *85*, 5262–5274.

Mascola, J.R., and Haynes, B.F. (2013). HIV-1 neutralizing antibodies: understanding nature's pathways. Immunol. Rev. *254*, 225–244.

Meyer-Hermann, M. (2002). A mathematical model for the germinal center morphology and affinity maturation. J. Theor. Biol. *216*, 273–300.

Meyer-Hermann, M.E., Maini, P.K., and Iber, D. (2006). An analysis of B cell selection mechanisms in germinal centers. Math. Med. Biol. *23*, 255–277.

Nieuwenhuis, P., and Opstelten, D. (1984). Functional anatomy of germinal centers. Am. J. Anat. *170*, 421–435.

Oprea, M., and Perelson, A.S. (1997). Somatic mutation leads to efficient affinity maturation when centrocytes recycle back to centroblasts. J. Immunol. *158*, 5155–5162.

Pancera, M., Zhou, T., Druz, A., Georgiev, I.S., Soto, C., Gorman, J., Huang, J., Acharya, P., Chuang, G.Y., Ofek, G., et al. (2014). Structure and immune recognition of trimeric pre-fusion HIV-1 Env. Nature *514*, 455–461.

Pantophlet, R., Wilson, I.A., and Burton, D.R. (2003). Hyperglycosylated mutants of human immunodeficiency virus (HIV) type 1 monomeric gp120 as novel antigens for HIV vaccine design. J. Virol. *77*, 5889–5901.

Pissani, F., Malherbe, D.C., Robins, H., DeFilippis, V.R., Park, B., Sellhorn, G., Stamatatos, L., Overbaugh, J., and Haigwood, N.L. (2012). Motif-optimized subtype A HIV envelope-based DNA vaccines rapidly elicit neutralizing antibodies when delivered sequentially. Vaccine *30*, 5519–5526.

Seaman, M.S., Janes, H., Hawkins, N., Grandpre, L.E., Devoy, C., Giri, A., Coffey, R.T., Harris, L., Wood, B., Daniels, M.G., et al. (2010). Tiered categorization of a diverse panel of HIV-1 Env pseudoviruses for assessment of neutralizing antibodies. J. Virol. *84*, 1439–1452.

Selvarajah, S., Puffer, B., Pantophlet, R., Law, M., Doms, R.W., and Burton, D.R. (2005). Comparing antigenicity and immunogenicity of engineered gp120. J. Virol. *79*, 12148–12163.

Shlomchik, M.J., and Weisel, F. (2012). Germinal centers. Immunol. Rev. *247*, 5–10.

Shlomchik, M.J., Watts, P., Weigert, M.G., and Litwin, S. (1998). Clone: a Monte-Carlo computer simulation of B cell clonal expansion, somatic mutation, and antigen-driven selection. Curr. Top. Microbiol. Immunol. *229*, 173–197.

Shulman, Z., Gitlin, A.D., Targ, S., Jankovic, M., Pasqual, G., Nussenzweig, M.C., and Victora, G.D. (2013). T follicular helper cell dynamics in germinal centers. Science *341*, 673–677.

Swerdlin, N., Cohen, I.R., and Harel, D. (2008). The lymph node B cell immune response: dynamic analysis in-silico. Proc. IEEE *96*, 1421–1443.

Thali, M., Furman, C., Ho, D.D., Robinson, J., Tilley, S., Pinter, A., and Sodroski, J. (1992). Discontinuous, conserved neutralization epitopes overlapping the CD4-binding region of human immunodeficiency virus type 1 gp120 envelope glycoprotein. J. Virol. *66*, 5635–5641.

Victora, G.D., and Nussenzweig, M.C. (2012). Germinal centers. Annu. Rev. Immunol. *30*, 429–457.

Victora, G.D., Schwickert, T.A., Fooksman, D.R., Kamphorst, A.O., Meyer-Hermann, M., Dustin, M.L., and Nussenzweig, M.C. (2010). Germinal center dynamics revealed by multiphoton microscopy with a photoactivatable fluorescent reporter. Cell *143*, 592–605.

Wagner, S.D., Milstein, C., and Neuberger, M.S. (1995). Codon bias targets mutation. Nature *376*, 732.

Walker, L.M., Huber, M., Doores, K.J., Falkowska, E., Pejchal, R., Julien, J.P., Wang, S.K., Ramos, A., Chan-Hui, P.Y., Moyle, M., et al.; Protocol G Principal Investigators (2011). Broad neutralization coverage of HIV by multiple highly potent antibodies. Nature *477*, 466–470.

Wedemayer, G.J., Patten, P.A., Wang, L.H., Schultz, P.G., and Stevens, R.C. (1997). Structural insights into the evolution of an antibody combining site. Science *276*, 1665–1669.

Wei, X., Decker, J.M., Wang, S., Hui, H., Kappes, J.C., Wu, X., Salazar-Gonzalez, J.F., Salazar, M.G., Kilby, J.M., Saag, M.S., et al. (2003). Antibody neutralization and escape by HIV-1. Nature *422*, 307–312.

West, A.P., Jr., Scharf, L., Scheid, J.F., Klein, F., Bjorkman, P.J., and Nussenzweig, M.C. (2014). Structural insights on the role of antibodies in HIV-1 vaccine and therapy. Cell *156*, 633–648.

Wyatt, R., Kwong, P.D., Desjardins, E., Sweet, R.W., Robinson, J., Hendrickson, W.A., and Sodroski, J.G. (1998). The antigenic structure of the HIV gp120 envelope glycoprotein. Nature *393*, 705–711.

Ye, L., Zeng, R., Bai, Y., Roopenian, D.C., and Zhu, X. (2011). Efficient mucosal vaccination mediated by the neonatal Fc receptor. Nat. Biotechnol. *29*, 158–163.

Zhang, J., and Shakhnovich, E.I. (2010). Optimality of mutation and selection in germinal centers. PLoS Comput. Biol. *6*, e1000800.

Zhou, T., Georgiev, I., Wu, X., Yang, Z.Y., Dai, K., Finzi, A., Kwon, Y.D., Scheid, J.F., Shi, W., Xu, L., et al. (2010). Structural basis for broad and potent neutralization of HIV-1 by antibody VRC01. Science *329*, 811–817.

EXTENDED EXPERIMENTAL PROCEDURES

Simulation Methods

We perform agent-based simulations of the GC reaction, treating individual B cells as discrete entities. The affinity of a BCR for Ag variants displayed on FDCs is obtained as described in the main text, with some further details provided below.

Discrete time is in units of GCR cycles (~2 GCR cycles per day). All the energies are in units of kcal/mol. But, it is important to note that all absolute values scale with the threshold affinity, E_a, defined in the main text. We treat a GC as an integrated compartment, where a series of maturation events occur during each GCR cycle. We do not explicitly consider any spatial structures of the GC or diffusion of cells.

Several key events occur which closely mimic the crucial processes of AM:

Activation

Each GC starts with 3 founder B cells (initial h sequences) which barely meet the activation threshold. We set the activation threshold as E_a = 10.8 kcal/mol, which might be somewhat higher than the actual value. But since all the energies scale with E_a, qualitative results should not depend on this number. If we broaden the affinity distribution of seeding cells to [E_a-kT, E_a+kT], the survival rate would be slightly higher, whereas the breadth remains similar, and the relative efficacy of various schemes is unchanged. Stronger variations in initial affinities would be biologically unlikely. The value of h on each site is randomly drawn from the interval [-0.18, 0.9]. Founder cells expand without mutation to $3 \times 2^9 = 1536$ cells.

Each GCR cycle proceeds in three main steps:

Replication-Dependent Mutation

Each BCR sequence replicates twice (on average 4 division/day and 2 cycle/day and so 2 division/cycle) during which mutation occurs with probability $\mu = 10^{-3} \times 3 \times N \cong 0.14$ per sequence per division (N = 46 is the total number of residues). We treat 3 types of point mutations as follows: (1) lethal mutation occurring with probability $p_L = 0.3$— remove the B cell; (2) silent mutation with probability $p_S = 0.5$— no change in $\vec{h}$; (3) affinity-affecting mutations with probability $p_A = 0.2$— randomly choose a site/residue k, draw a value of affinity change ΔE from the asymmetric distribution $P(\Delta E)$ (Figure S1A) and convert it into a *change* of the interaction strength Δh_k with the chosen residue via $\Delta E = \Delta h_k \cdot s_k$, where s_k is the identity of that residue on the Ag epitope, and then update the interaction strength h_k to $h_k' = h_k + \Delta h_k$. If residue k makes contacts with conserved residues of the epitope, nothing else happens. If residue k interacts with an epitope residue that shields the conserved residues, a residue on the paratope that interacts with a conserved residue on the epitope is randomly chosen, and the value of h corresponding to this residue is changed according to: $h' = h - \alpha(|h_k'| - |h_k|)$, where the resulting h' is bounded between $[-1.5,1.5]$, a broader range than that of the seeding cells and assumed symmetric for simplicity/generality. So if the strength of an interaction with a residue that masks the epitope is reduced (i.e., $|h_k'| < |h_k|$), there is an affinity enhancement, i.e. $-\alpha(|h_k'| - |h_k|) > 0$, and an affinity reduction if the interaction is strengthened. For paratope residues that interact with mutated variable residues, an identical procedure is followed, except that the resulting h' is only lower bounded by -1.5 and has no upper bound. To compare the efficacy of various immunization protocols in eliciting bnAbs, we assume a relatively large value of α ($\alpha = 2$) in all the presented studies. A large value of α effectively amplifies the size of potentially beneficial mutations and encourages the emergence and selection of cross-reactive antibodies.

Affinity-Dependent Selection

B cells that do not carry lethal mutations compete for selection. They can survive the static threshold E_a with a probability P_a (Equation 1 in Experimental Procedures). B cells that successfully internalize Ag then compete for T cell help, with a probability P_{Th} (Equation 2 in Experimental Procedures) of getting selected. Both probabilities depend on the affinity of the B cell for the FDC Ag it sees. The competing subpopulation that determines the probability of receiving T cell help involves only contemporary B cells for the "peers only" case, while for the "Ab feedback" scenario it also includes all the Abs produced in previous rounds of maturation. Abs compete with GC B cells for binding to Ag displayed on FDCs. This provides a competitive disadvantge to B cells with BCRs that bind weakly to Ag compared to those that bind more strongly. Within our formulation, this is effectively incorporated in Equation 2. If each B cell interacts with only one type of Ag during each binding attempt, there is no sum over j in Equations 1 and 2, and the encountered Ag type for each B cell is randomly picked in every round of selection. This procedure reflects the heterogeneity of Ag distribution on the FDCs as well as the non-specificity of T cell help with respect to the viral epitopes that B cells target.

Recycle and Output

Selected B cells are recycled to enter the next GCR cycle with a probability $p_r = 0.9$. Otherwise, they are stored and accumulated as memory cells and antibody-secreting cells in equal amount; secreted antibodies come back to compete in the selection cycle in the "Ab feedback" scenario.

Termination

We set a maximum duration, t_i^{max}, for each maturation period i (i.e., following each Ag administration) during which the concentration and display of FDC Ag remain the same: scheme I (WT+v1+v2):$t_1^{max} = 240$, scheme II (WT|v1+v2): $t_1^{max} = 80$, $t_2^{max} = 160$, and scheme III (WT|v1|v2): $t_i^{max} = 80$, i = 1,2,3. Once a GC reaches the threshold size of about 1,500 cells or the maximum duration of the current period, it jumps to the next period. The assumed duration or time interval between successive injections is sufficiently long for the GC to recover the initial number of B cells after each dose in the most efficient scheme (WT|v1|v2). GCR terminates if the B cell population size hits zero or the final period is finished.

For simplicity, the concentration of FDC Ag during each maturation period is assumed to be constant, and the total concentration, C_{tot}, of each dose is taken to be identical. This dimensionless number indicates the relative abundance of Ag molecules with respect to maturing B cells that interact with the FDCs. To demonstrate the relative efficacy of various schemes, we choose the values of C_{tot} that correspond to a near optimal breadth. In the case of scheme III, this would lead to a low survival rate, and so, the chosen concentration is slightly higher, but still maintains large breadth. These values are listed in Table 1 and used in the figures. Survival rate and average breadth over the whole relevant range of Ag concentrations for each scheme are displayed in Figure S4 (scheme I) and Figure 2 (schemes II and III). We choose the neutralization threshold E_{nt} = 11.3 kcal/mol to be slightly higher than E_a. Using larger values of E_{nt} will not alter the qualitative difference between various schemes (data not shown).

Each simulation trajectory represents a single GC. To quantify the efficacy of different strategies, we simulate a large ensemble of GCs (several thousand for each scheme) and examine the statistics of various characteristics. Quantities we keep track of for each GC include: the history of selecting Ag variants for each surviving B cell, the average interaction strength with conserved (h_c) and variable (h_v) residues, the affinity of recycled B cells for each type of FDC Ag, the time-varying GC size and the GCR duration, as well as the clone-averaged breadth and number of mutations accumulated over time. For the GC ensembles, results are presented as distributions (histograms) of clone-averaged breadth and interaction strength (h_c and h_v) observed at the end of the simulations. Histograms show the relative abundance of GCs having different values of the measure in different simulation runs. The survival rate of GCs is defined as the fraction of GCs that do not go extinct within the maximum total duration.

Experimental Procedures

Display of gp120 on Yeast

Genes for gp120 constructs were subcloned into the yeast display vector pCHA between NheI and BamHI restriction sites, immediately downstream of an HA epitope tag (YPYDVPDYA) and upstream of a CMyc tag (EQKLISEEDL) and the Aga-2 fusion partner. The protein was displayed on *Saccharomyces cerevisiae* strain EBY100 using a standard surface display protocol (Chao et al., 2006). In brief, transformed yeast were grown to mid-log phase in SD-CAA media at 30°C, and induced in galactose-containing SG-CAA media for 24 hr at 20°C. Approximately 10^5 gp120 molecules are displayed per yeast, as measured by quantitative flow cytometry (data not shown).

Library Construction and Sorting

Degenerate oligonucleotide primers (Integrated DNA Technologies, Coralville, IA) were designed to introduce diversity at selected positions while maintaining overlapping homology with each other. Eleven fragments were amplified with these degenerate primers by PCR for 30 cycles with Taq polymerase (New England Biolabs, Ipswich, MA) and purified by gel electrophoresis. The full-length gene was reconstituted by pairwise overlap-extension PCR of these fragments. Each reaction consisted of 8 self-priming cycles with adjacent oligonucleotide fragments, followed by 30 cycles with primers homologous to the termini. The amplified product was purified by gel electrophoresis and re-amplified with outer primers for an additional 30 cycles. The full-length library was transformed into yeast by electroporation.

The induced library was incubated with VRC01 (expression plasmids a generous gift from John Mascola, Vaccine Research Center, NIAID, NIH) at the stated concentration and chicken anti-CMyc at 10-fold molar excess (Gallus Immunotech, Fergus, Ontario). Secondary labeling was perfumed with Alexa Fluor-labeled goat anti-human and goat anti-chicken antibodies (Life Technologies, Carlsbad, CA) at recommended dilutions. The library was sorted on a MoFlo instrument (Beckman Coulter, Brea, CA).

Secretion of Fc-gp120 from HEK293 cells

gp120 constructs were subcloned into a mammalian expression vector based on gWiz (Genlantis, San Diego, CA) downstream of the Fc domain of mouse IgG2a and a his6 tag. A suspension culture of HEK293 cells grown in serum-free medium (Freestyle 293, Life Technologies, Carlsbad, CA) was transfected with DNA using PEI as per manufacturer's instructions. Supernatant was harvested after one week and purified by sequential metal affinity chromatography (TALON resin, Clontech, Mountain View, CA) and protein A affinity chromatography (Genscript, Piscataway, NJ).

Yeast Cell Surface Binding Assays

Cell surface binding titrations were performed with various combinations of displayed and soluble proteins, e.g., displayed gp120 binding to soluble anti-gp120 antibodies or serum from immunized mice; displayed VRC01 scFv binding to soluble gp120. In all instances, display was detected by chicken anti-CMyc (Gallus Immunotech, Fergus, Ontario). Secondary labeling was performed with Alexa Fluor-labeled goat anti-human or anti-mouse, and goat anti-chicken antibodies (Life Technologies, Carlsbad, CA) at a 1:400 dilution, and analyzed on a FACSCalibur HTS with a high-throughput plate sampler (Becton Dickinson, Franklin Lakes, NJ).

Immunizations

Experiments were performed on 6-8 week-old female BALB/c mice (Taconic, Hudson, NY). Animals were treated in accordance with guidelines set forth by the Committee on Animal Care of the MIT Division of Comparative Medicine. Animals were immunized intranasally in the method described by Zhu and colleagues (Ye et al., 2011). Briefly, animals were administered 50 pmol Fc-gp120 (6 μg total protein, or 3 μg gp120 equivalents) intranasally with 3 nmol CpG-1826 adjuvant (Integrated DNA Technologies, Coralville, IA) in PBS. The maximum administered volume was 15 μL. Mice were boosted at two-week intervals, and serum was collected weekly in Microtainer serum separator tubes with thrombin-based clot activator and polymer gel (Becton Dickinson, Franklin Lakes, NJ).

Analysis of Serum Binding

Antisera were titrated on gp120-displaying yeast. In each well of a 96-well plate, $1.5x10^4$ induced yeast were incubated with serial dilutions of serum and 40 ng chicken anti-CMyc (Gallus Immunotech, Fergus, Ontario) in 50 μl for several hours. Secondary labeling

was performed with Alexa Fluor-labeled goat anti-human and goat anti-chicken antibodies (Life Technologies, Carlsbad, CA) at a 1:400 dilution, and analyzed on a FACSCalibur HTS with a high-throughput plate sampler (Becton Dickinson, Franklin Lakes, NJ).

Median binding signals were fit using MATLAB (MathWorks, Natick, MA) to a monovalent binding isotherm of the form $y = y_{max}\ dil^{-1}/(dil^{-1} + K_A^{-1})$ where "dil" is the serum dilution and y is the binding signal in MFU. The two fitted parameters are the maximal binding signal, y_{max}, which can depend upon the number of antibodies able to simultaneously bind a particular gp120 variant displayed on yeast, and the apparent equilibrium association constant, K_A. The precise relationship between K_A and antibody affinity is difficult to elucidate, as the apparent affinity value is confounded by the fact that the assay is performed on a polyclonal mixture of antibodies. However, K_A can be understood to be a combination measure of the affinity and number of antigen-specific antibodies in the serum. For the sera in Figure 5C–5E of the main text, the fitted apparent affinity parameter K_A (reported as fold dilution) is as follows: (C) Sequential: $K_{A\text{-Core}} = 1830$, $K_{A\text{-Clone A}} = 1240$, $K_{A\text{-Clone B}} = 1630$, $K_{A\text{-Clone C}} = 1735$; (D) Parallel: $K_{A\text{-Core}} = 2600$, $K_{A\text{-Clone A}} = 230$, $K_{A\text{-Clone B}} = 210$, $K_{A\text{-Clone C}} = < 100$; (E) core only: $K_{A\text{-Core}} = 600$, $K_{A\text{-Clone A}} = < 100$, $K_{A\text{-Clone B}} = < 100$, $K_{A\text{-Clone C}} = < 100$. K_A is a combination measure of the affinity and number of antigen-specific antibodies in the serum, but the polyclonal nature of the serum precludes a precise relationship between K_A and antibody affinity.

Ternary Complex Assay

This assay, a yeast-based "sandwich ELISA," has two iterations. In the first, an excess of serum at a saturating dilution (as calculated by cell-surface titration) is incubated with soluble stripped core (not an Fc-fusion) at 4°C overnight. This solution (20 nM gp120) is then added to $5x10^4$ yeast displaying the scFv of VRC01 in a 96-well plate and incubated for 1 hr at 4°C. In the second iteration, yeast displaying the scFv of VRC01 are incubated with a > 10x molar excess of 20 nM soluble stripped core at 4°C overnight. The yeast are washed and distributed into a 96-well plate at $5x10^4$ cells per well. Serum is added at a saturating dilution and the plate is incubated for 1 hr at 4°. The formation of a ternary complex—a sandwich of VRC01, gp120, and mouse serum—is detected by secondary labeling with goat anti-mouse 647 (Life Technologies, Carlsbad, CA) at a 1:400 dilution, and analyzed on a FACSCalibur HTS with a high-throughput plate sampler (Becton Dickinson, Franklin Lakes, NJ).

Display of Stripped Core gp120 on Yeast

The display of a stripped core gp120 on yeast has been described previously (Mata-Fink et al., 2013). Briefly, full-length gp120 from HIV strain YU2 (GenBank Accession number M93258) (Li et al., 1992) was modified by removing the flexible gp41-interactive regions at the N- and C-termini (aa 1-89, 493-511) (Pancera et al., 2010; replacing the hyper-variable loops V1/V2 (aa 124-198), V3 (aa 298-329), and the bridging sheet β20/21 (aa 422-437) with short glycosylated amino acid linkers; and introducing an N-linked glycosylation sequence at amino acid 114, a site previously identified as important for masking an epitope on the V1/V2 stem (Pantophlet et al., 2003) (Table S1). These modifications are similar, though not identical, to those in the original core gp120 crystalized in complex with CD4 (Kwong et al., 1998). The gene for stripped core gp120 was subcloned into a yeast display vector with a C-terminal Aga2p fusion partner. The protein expresses well on the yeast surface ($1x10^5$ copies per cell; standard for yeast surface display) and conserves the structure of the CD4 binding site as measured by binding to CD4 and to a panel of neutralizing antibodies (Mata-Fink et al., 2013).

Generation of Surface-Diversified Immunogens by Semi-Random Mutagenesis

Our previous experience with mutagenesis of yeast-displayed stripped core gp120 for epitope mapping suggested that the conformational CD4 binding site is sensitive to allosteric mutations that disrupt the overall fold of the molecule. Immunogen diversity was therefore focused on likely surface residues. A homology model of stripped core gp120 was generated with the protein structure modeling program MODELER (http://salilab.org/modeller) (Sali and Blundell, 1993), and 43 evenly-spaced, solvent-exposed surface residues not in the CD4 binding site were selected for diversification (Table S1). Diversity was introduced by PCR with degenerate oligonucleotide primers. Regions of the gp120 gene were amplified with primers containing random nucleotides (NNB) at chosen positions, and then pieced together by overlap-extension PCR to reconstitute the full gene. The library of $5x10^7$ unique clones was transformed into yeast and induced for display by standard methods (Chao et al., 2006). The library was screened twice by FACS for binding to 10 nM then 50 nM VRC01 to enrich for clones that retained correct presentation of the CD4 binding site (Figure S6A). Based on the degree of library oversampling (2.35x) and percentage of cells isolated at each sort (0.0067% and 7.1%, respectively), we estimate that 200-500 unique clones were collected (Firth and Patrick, 2005; Patrick et al., 2003). Plasmid DNA from sorted cells was isolated and 288 variants were sequenced. 20 mutants with high diversity were then secreted from HEK293 cells as mouse Fc fusions, purified by sequential metal affinity and protein A chromatography, and tested for binding to VRC01 scFv displayed on yeast. Many of the secreted mutants were unstable and degraded over a few days, but three gp120 variants that were stable and retained binding to VRC01 in this format were selected as candidate immunogens (Figure S6B). Fitted K_D values were 3.5 nM (stripped core), 6.2 nM (clone A), 1.5 nM (clone B), and 12.2 nM (clone C).

Characterization of Variant Immunogens

The full amino acid sequences of the four candidate immnogens—stripped core gp120 and the three diversified variants, henceforth called clones A, B, and C—were analyzed. 43 of 285 amino acids were diversified, with a pairwise sequence identity of 13.6% at these positions (Table S1). The CD4 binding site-directed antibodies VRC01, b12, and b13 were titrated against the individual immunogens displayed on yeast (Figures S6C–S6F). VRC01 neutralizes greater than 90% of circulating HIV isolates (Wu et al., 2010). Antibody b12 is CD4-competitive but is neither as potent nor as broadly cross-reactive as VRC01 (Burton et al., 1991; Burton et al., 1994). Antibody b13 also binds the CD4 binding site on monomeric gp120, but is unable to bind trimeric envelope on HIVand is thus incapable of

neutralizing the virus (Chen et al., 2009). Yeast-displayed stripped core binds with similar affinity to all three antibodies, whereas the mutants exhibit varying degrees of weaker binding to b12 and b13 against which they were not sorted.

Analysis of Monoclonal Antibodies from Immunized Mouse

A sequentially immunized mouse was sacrificed and hybridomas generated by splenocyte fusion (Green Mountain Antibodies, Burlington VT). Two clones were isolated by screening for binding to stripped core gp120 by ELISA and by yeast cell surface titration. The specificities of the monoclonal antibodies were assessed by binding to the D368R mutant gp120 displayed on yeast, and by the ternary complex assay described above. The sequence identities of these clones was assessed by PCR of cDNA from the hybridoma. Isotype analysis was performed by ELISA. The monoclonal antibody sequences were as follows:

Monoclonal Antibody Clone	mAb-1	mAb-2
Isotype	IgG2a	IgG1
CDRH1	FSLSTSGVGVG	YTFTNYGMN
CDRH2	HIWWDDDRRYNPALKS	WINTYTGEPTYGDDFKG
CDRH3	IRYGSRYGMDY	GDYDGDWFAY
CDRL1	RASESVEYYVTSLMQ	KASQSVSNDVA
CDRL2	AASNVES	YASNRYT
CDRL3	QQSKKVPFTFGGG	QQDYGSPWTFGGG

SUPPLEMENTAL REFERENCES

Burton, D.R., Barbas, C.F., 3rd, Persson, M.A., Koenig, S., Chanock, R.M., and Lerner, R.A. (1991). A large array of human monoclonal antibodies to type 1 human immunodeficiency virus from combinatorial libraries of asymptomatic seropositive individuals. Proc. Natl. Acad. Sci. USA *88*, 10134–10137.

Burton, D.R., Pyati, J., Koduri, R., Sharp, S.J., Thornton, G.B., Parren, P.W., Sawyer, L.S., Hendry, R.M., Dunlop, N., Nara, P.L., et al. (1994). Efficient neutralization of primary isolates of HIV-1 by a recombinant human monoclonal antibody. Science *266*, 1024–1027.

Chao, G., Lau, W.L., Hackel, B.J., Sazinsky, S.L., Lippow, S.M., and Wittrup, K.D. (2006). Isolating and engineering human antibodies using yeast surface display. Nat. Protoc. *1*, 755–768.

Chen, L., Kwon, Y.D., Zhou, T., Wu, X., O'Dell, S., Cavacini, L., Hessell, A.J., Pancera, M., Tang, M., Xu, L., et al. (2009). Structural basis of immune evasion at the site of CD4 attachment on HIV-1 gp120. Science *326*, 1123–1127.

Firth, A.E., and Patrick, W.M. (2005). Statistics of protein library construction. Bioinformatics *21*, 3314–3315.

Korber, B., Foley, B., Kuiken, C., and Pillai, S. (1998). Numbering positions in HIV relative to HXB2CG. LANL Human Retroviruses and AIDS Compendium *1998*, 102–111.

Kwong, P.D., Wyatt, R., Robinson, J., Sweet, R.W., Sodroski, J., and Hendrickson, W.A. (1998). Structure of an HIV gp120 envelope glycoprotein in complex with the CD4 receptor and a neutralizing human antibody. Nature *393*, 648–659.

Li, Y., Hui, H., Burgess, C.J., Price, R.W., Sharp, P.M., Hahn, B.H., and Shaw, G.M. (1992). Complete nucleotide sequence, genome organization, and biological properties of human immunodeficiency virus type 1 in vivo: evidence for limited defectiveness and complementation. J. Virol. *66*, 6587–6600.

Mata-Fink, J., Kriegsman, B., Yu, H.X., Zhu, H., Hanson, M.C., Irvine, D.J., and Wittrup, K.D. (2013). Rapid conformational epitope mapping of anti-gp120 antibodies with a designed mutant panel displayed on yeast. J. Mol. Biol. *425*, 444–456.

Pancera, M., Majeed, S., Ban, Y.E., Chen, L., Huang, C.C., Kong, L., Kwon, Y.D., Stuckey, J., Zhou, T., Robinson, J.E., et al. (2010). Structure of HIV-1 gp120 with gp41-interactive region reveals layered envelope architecture and basis of conformational mobility. Proc. Natl. Acad. Sci. USA *107*, 1166–1171.

Patrick, W.M., Firth, A.E., and Blackburn, J.M. (2003). User-friendly algorithms for estimating completeness and diversity in randomized protein-encoding libraries. Protein Eng. *16*, 451–457.

Sali, A., and Blundell, T.L. (1993). Comparative protein modelling by satisfaction of spatial restraints. J. Mol. Biol. *234*, 779–815.

Wu, X., Yang, Z.Y., Li, Y., Hogerkorp, C.M., Schief, W.R., Seaman, M.S., Zhou, T., Schmidt, S.D., Wu, L., Xu, L., et al. (2010). Rational design of envelope identifies broadly neutralizing human monoclonal antibodies to HIV-1. Science *329*, 856–861.

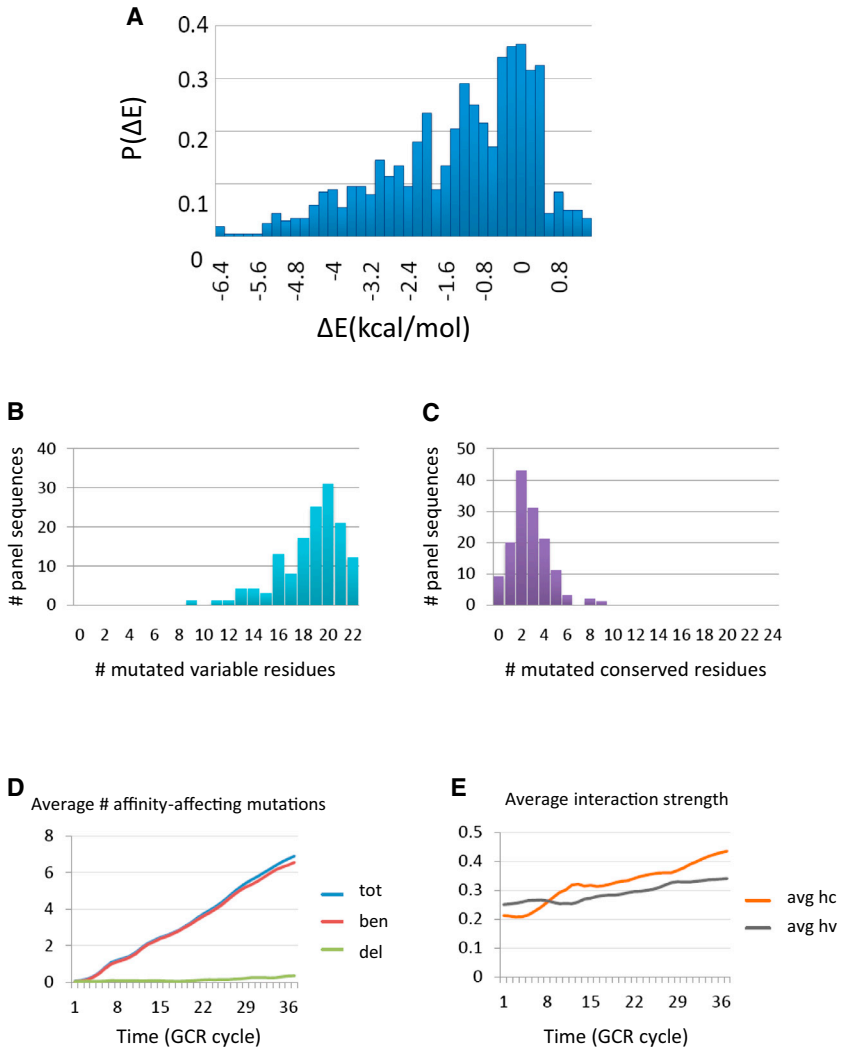

Figure S1. Details of In Silico Model

(A) Histogram of affinity change due to point mutations. Adapted from Figure 1 of Zhang and Shakhnovich (2010). Here, the bin size is 0.2 kcal/mol. Only 5% of mutations could improve affinity.

(B and C) Characteristics of the virus panel used for assessment of neutralizing antibodies. Shown are the distributions of the number of mutated variable residues (B) and mutated conserved residues (C) for the 141 test panel sequences. The vast majority of the panel sequences have nearly 20 mutated variable residues, and yet remain viable. Conserved residues of the epitope indeed have a very modest mutability.

(D and E) Characteristics of affinity maturation against a single antigen. (D) Average number of affinity-affecting mutations in recycled B cells as a function of time (in units of GCR cycles). Red for beneficial mutations, green for deleterious ones, and blue for total. (E) Time evolution of the residue- and clone-averaged interaction strength of recycled B cells with the conserved (avg h_c) and variable (avg h_v) residues of the antigen.

Related to main Figure 1.

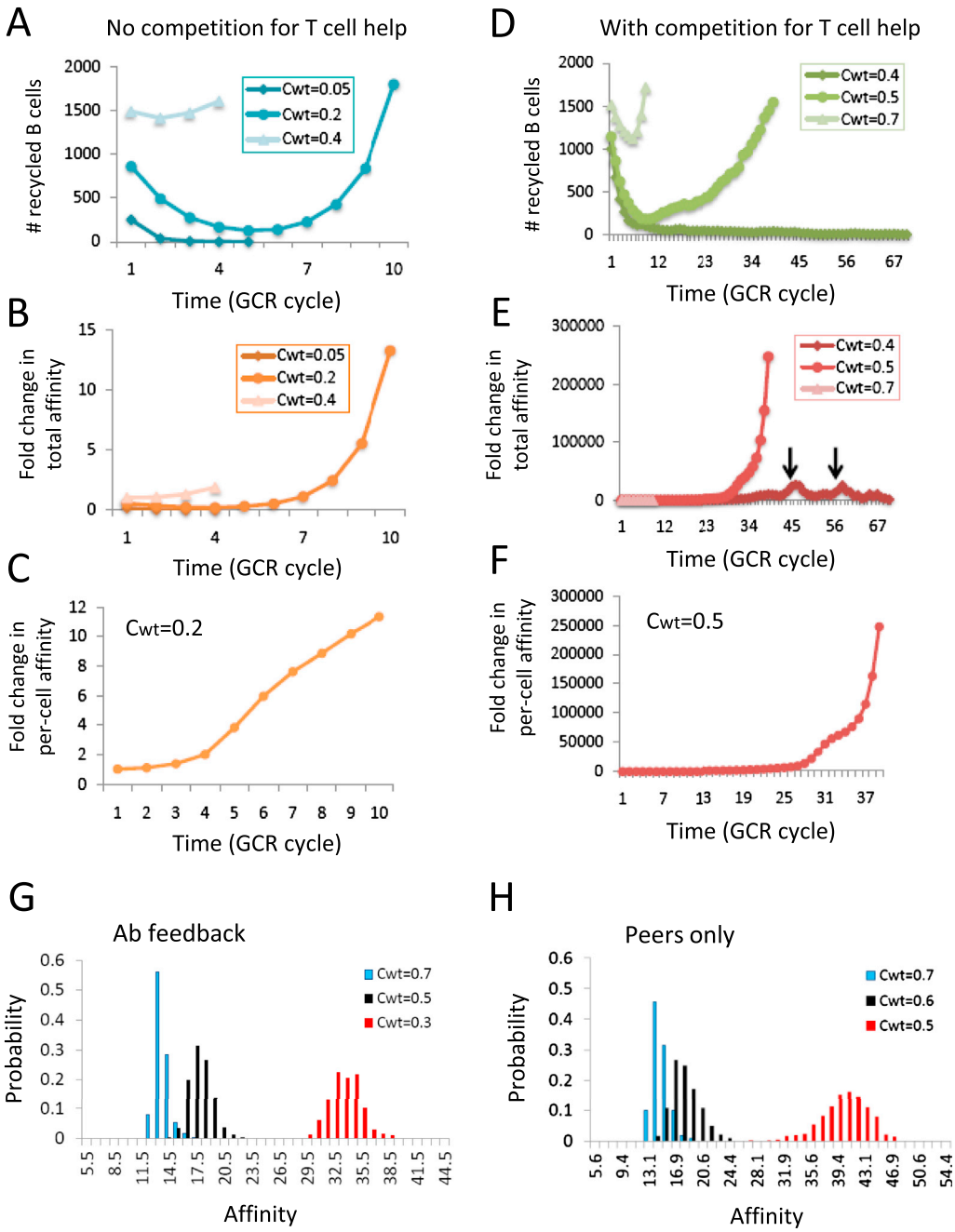

Figure S2. Concentration Dependent Evolution of Antibody Affinities for a Single Antigen

(A–F) Existence of an optimal dosage of stimulating antigen for effecitve affinity maturation. Shown are the number of recycled B cells (A and D) and the corresponding fold change in total affinity (B and E) and clonal affinity (C and F) as a function of time, at various antigen concentrations (C_{wt}). Identical seeding B cells are used in all the cases. The total affinity at time t is defined as $\sum_{i=1}^{n_B(t)} \exp[E_i(t)/k_BT]$, where $E_i(t)$ is the binding affinity of B cell clone i to the wild-type antigen at time t and $n_B(t)$ is the total number of recycled B cells in cycle t. The fold change is given by the ratio of current to initial values. (A-C) No competition for T cell help, i.e., only a static threshold (Equation 1 in Experimental Procedures) for selection. Increase in clonal affinity slows down once the population passes the bottleneck and starts fast growth (C). (D–F) With competition for T cell help, i.e., selected B cells have to exceed a dynamic threshold (Equation 2 in Experimental Procedures) which typically increases with GC cycles. Steep increase in clonal affinity persists even after the population starts expanding rapidly (F).

(G and H) Distribution of antibody affinities at various antigen concentrations. 500 trajectories for each concentration value C_{wt}. The presented affinity profile is obtained by averaging the final affinity distribution of matured B cells over the surviving GCs. "Ab feedback" (G) and "peers only" (H) scenarios for T-help competition. The profile broadens and shifts to higher affinity values as antigen concentration decreases.

Related to main Figure 2.

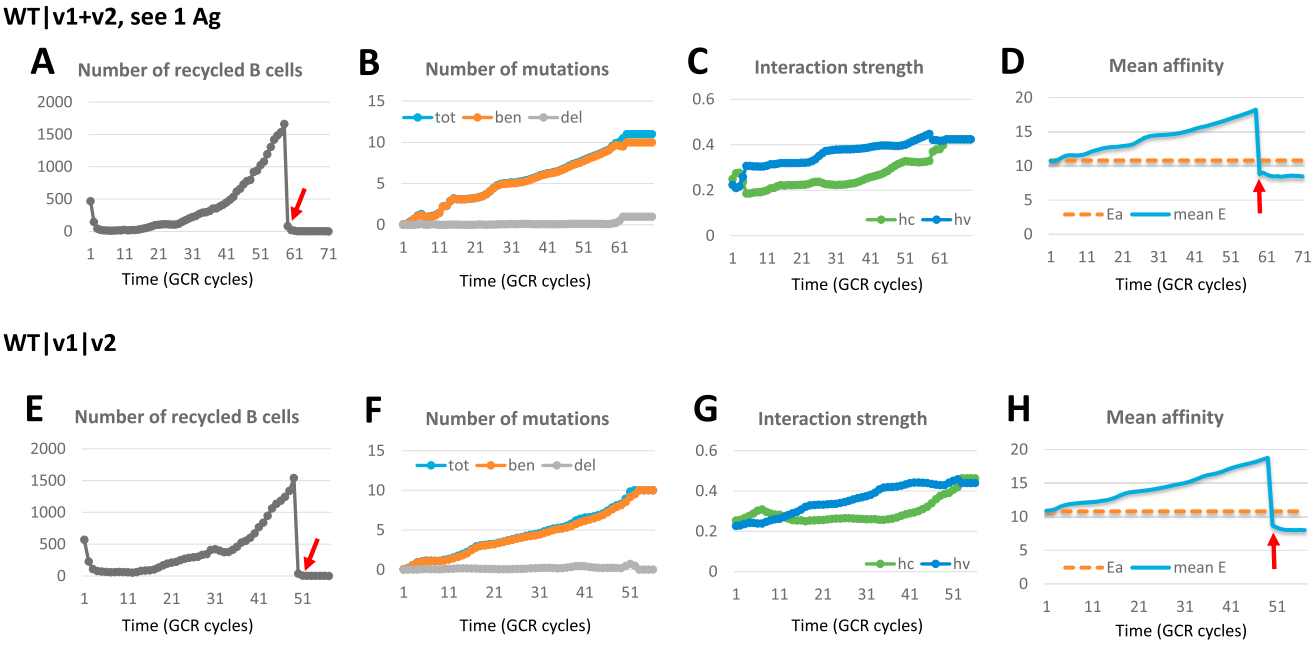

Figure S3. GC Collapse at High Ag Concentrations in "WT First" Schemes

(A–H) Shown are the temporal trajectories of maturation characteristics in schemes II (A–D) and III (E–H). Average breadth is zero in both cases. GC collapse (red arrow in A and E) upon encounter of the variant(s) due to failure of activation (red arrow in D and H), i.e., mean affinity falling below the activation threshold E_a. This occurs because maturation against WT Ag finishes quickly, only a small number of beneficial mutations accumulate (orange curve in B and F) and the interactions with the conserved residues (h_c) remain weak (green curve in C and G). Related to main Figure 2.

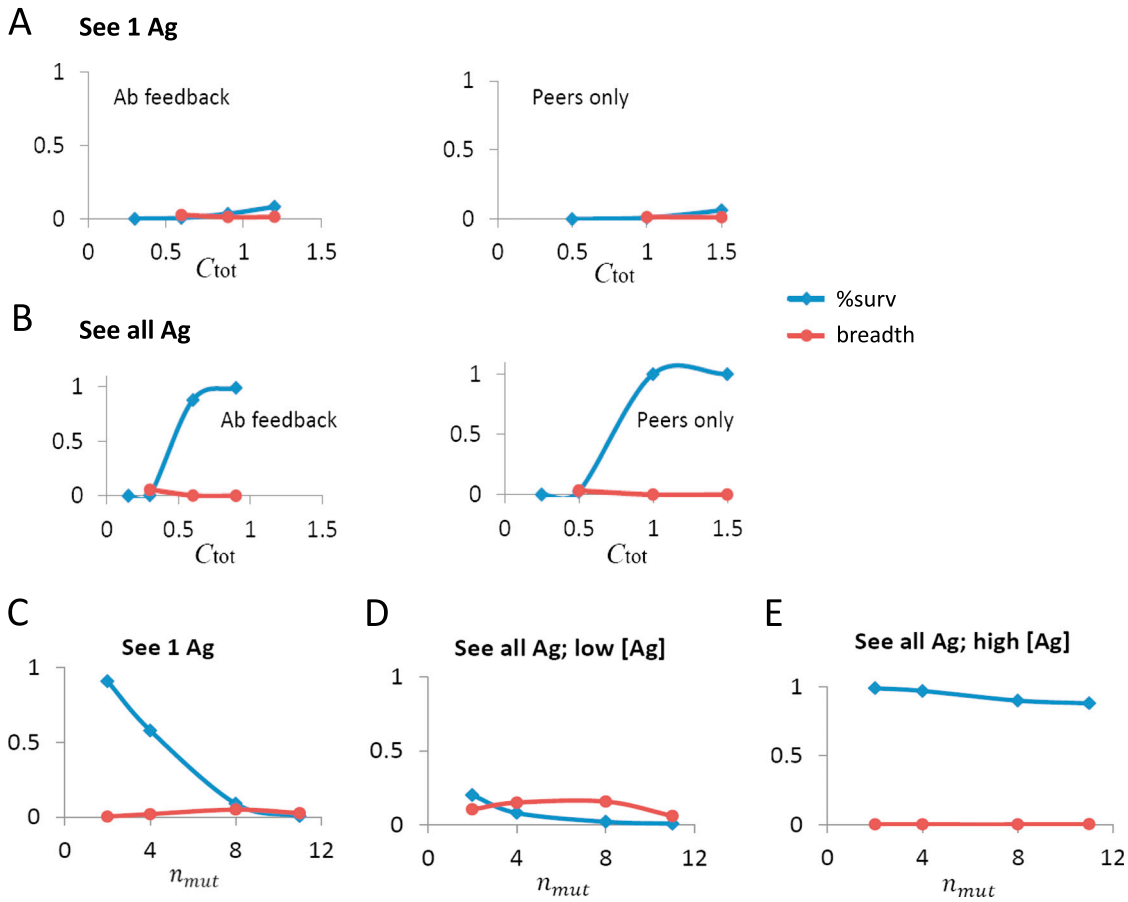

Figure S4. GC Survival and Antibody Breadth in Scheme I—WT+v1+v2

(A and B) Dependence on antigen concentration (C_{tot}). Results are shown for (A) see 1 Ag and (B) see all Ag scenarios with all (left column) or none (right column) of the secreted Abs participating in the T-help competition. The breadth is averaged over the surviving trajectories. Several thousand runs are performed for each value of C_{tot}.

(C–E) Dependence on the mutational distance (n_{mut}) between the antigen variants. Results are shown for (C) see 1 type of Ag, (D) see all types of Ag at lower concentrations than in (C), and (E) see all types of Ag at the same concentrations as in (C). All the Abs produced in earlier rounds of maturation join the competition for T cell help. If only peers compete for T cell help, GCs either die or end with essentially zero breadth. The breadth is averaged over the surviving trajectories out of 500 runs for each value of n_{mut}. Related to main Figure 3.

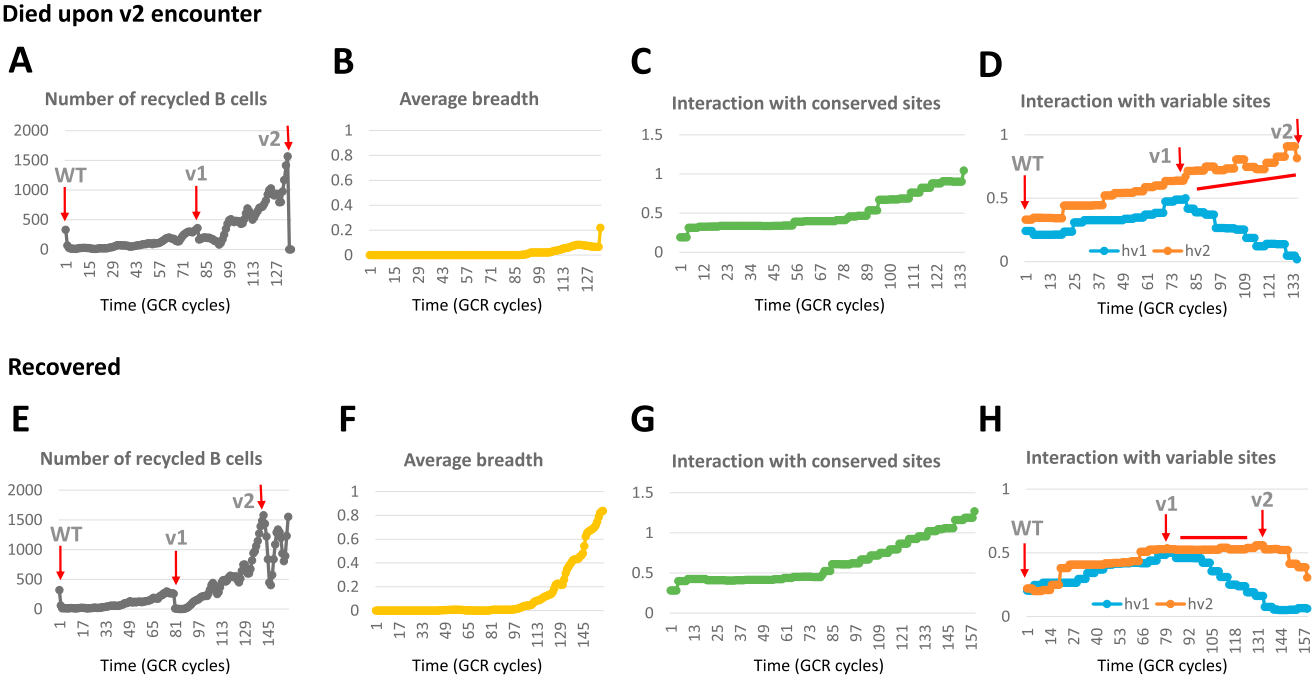

Figure S5. Two Main Lineages that Evolve in Scheme III—WT|v1|v2

(A–H) Shown are the temporal trajectories of maturation characteristics of the two main types of lineages. One lineage (A–D) enhances interactions with unmutated residues on the first variant (ascending h_{v2} in D) and extinguishes upon encounter of the second variant (A). The other (E–H) reduces interactions with the mutated residues/insertions on the two variants sequentially (descending h_{v1} and h_{v2} in H) thus further focusing interactions with the conserved residues (G). The latter recovers the initial population size (E) and develops a large breadth (F) at the end of maturation, whereas the former collapses (A) before breadth evolves (B). Related to main Figure 4.

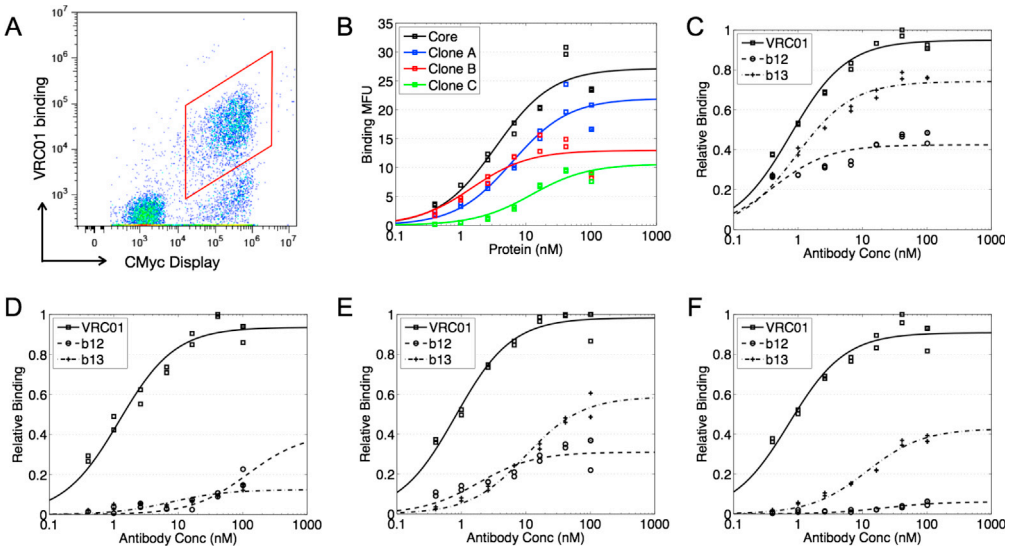

Figure S6. Generation and In Vitro Analysis of Diversified Immunogens

(A–F) As described in the text, the library of gp120 variants was displayed on yeast and sorted twice for binding to 50 nM VRC01. (A) FACS plot of the second library sort against VRC01. Clones in the red gate were collected and sequenced. Selected clones were secreted from HEK293 cells as fusions to mouse Fc. (B) Titration of stripped core and candidate immunogens (clones A–C) on yeast displaying VRC01 scFv. Fitted K_D values are 3.5 nM (stripped core), 6.2 nM (clone A), 1.5 nM (clone B), and 12.2 nM (clone C). (C–F) CD4 binding site-directed antibodies VRC01 (solid line), b12 (dashed line), and b13 (dash-dotted line) were titrated on yeast displaying (C) stripped core, (D) clone A, (E) clone B, or (F) clone C. An anti-c-Myc antibody was used to confirm display, and secondary detection was performed with fluorescently labeled anti-chicken and anti-mouse antibodies. Related to main Figure 5.